[13]. Consistent with these results, *Mgmt*$^{-/-}$ *Mlh1*$^{-/-}$ cells, derived from the gene-targeted mice, are unable to induce apoptosis and show an elevated mutant frequency after MNU treatment [14].

The apoptotic signal initiated through the mismatch recognition complex activates a signaling cascade leading to the cell cycle checkpoints and apoptotic pathways for cell death. Both the release of cytochrome C from the mitochondria as well as the activation of Apaf-1 and caspase-3, hallmarks of the induction of apoptosis, have been demonstrated after the treatment of cells with alkylating agents that produce O^6-methylguanine [14,15]. However, the precise molecular mechanism underlying the signal transduction downstream of mismatch recognition still remains to be determined. To identify the factors involved in the O^6-methylguanine-induced apoptotic process, we screened MNU-resistant clones derived from MNU-sensitive *Mgmt*$^{-/-}$ cells using retrovirus-mediated gene-trap mutagenesis [16]. Mouse-derived KH101 cells, carrying an insertional mutation in one of the alleles of an uncharacterized gene, were unable to induce mitochondrial membrane depolarization as well as caspase-3 activation, after treatment with MNU. In this way, we identified a new gene, designated as *Mapo1* (O^6-methylguanine induced apoptosis 1), which was related to the induction of apoptosis. The mutant frequency of KH101 cells was significantly elevated after the treatment with MNU, thus supporting the notion that the induction of apoptosis, in which the MAPO1 is involved, contributes significantly to the elimination of cells carrying mutation-inducing DNA lesions. A search in the database revealed that the amino acid sequence of the MAPO1 protein is homologous to that of folliculin-interacting protein 1 (FNIP1), which was identified as a protein having the capacity to associate with folliculin [17]. Folliculin is a tumor suppressor protein with unknown biological activity, and is encoded by the *FLCN* gene. Mutations in the *FLCN* gene have been found in patients with Birt-Hogg-Dubé (BHD) syndrome [18,19], which is characterized by the development of hair follicle hamartomas, lung cysts, and an increased risk for renal neoplasia [20–22]. Identification of another folliculin-interacting protein, displaying a similarity in its amino acid sequence to that of FNIP1, was reported by two groups of researchers and the gene responsible was named *FNIP2* and *FNIPL*, respectively [23,24]. The *FNIP2/FNIPL* gene turned out to be the same gene as the human homolog of *Mapo1*. It was also reported that FNIP2/FNIPL, as well as FNIP1, could bind to 5′-AMP-activated protein kinase (AMPK), composed of AMPKα, β and γ subunits, which is an important energy sensor in cells that negatively regulates cell growth and proliferation [25,26].

We report here that a complex composed of MAPO1, FLCN and AMPK is involved in the induction of apoptosis triggered by O^6-methylguanine–thymine mispair. Evidence is presented which shows that during the course of apoptosis induction, the phosphorylation of AMPKα occurs in a MAPO1- and FLCN-dependent manner.

2. Materials and methods

2.1. Cell lines and cell culture

The YT102 (*Mgmt*$^{-/-}$ *Mlh1*$^{+/+}$), YT103 (*Mgmt*$^{-/-}$ *Mlh1*$^{-/-}$) and KH101 (*Mgmt*$^{-/-}$ *Mapo1*$^{+/-}$) cell lines were established as described previously [14,16]. The cells were cultivated in Dulbecco's modified Eagle's medium (D-MEM) supplemented with 10% fetal bovine serum (FBS) at 37 °C in 5% CO_2.

2.2. Chemicals

N-Methyl-*N*-nitrosourea (MNU) was obtained from Sigma. Compound C and AICA-Ribose were purchased from Calbiochem.

2.3. Immunoprecipitation and immunoblotting

To prepare cells expressing Flag-tagged MAPO1 or HA-tagged FLCN, a pIRES-puro3 vector (Clontech) containing mouse-derived *Mapo1* cDNA tagged with Flag epitope at the carboxy terminal end or a pIRES-puro2 (Clontech) vector carrying mouse-derived *Flcn* cDNA tagged with the HA epitope at the amino terminal end was introduced into YT102 cells using Lipofectamine 2000 (Invitrogen) according to the manufacturer's protocol. For the immunoprecipitation, the cells were lysed with NETN buffer (50 mM Tris/HCl (pH 8.0), 150 mM NaCl, 0.2% NP-40, 1 mM EDTA) containing protease inhibitors (Roche). To precipitate the Flag-tagged MAPO1, 10 μl of anti-FLAG M2-agarose (Sigma) were added to the extract, and incubated for 4 h at 4 °C. Alternatively, 10 μl of anti-HA (HA-7)-agarose (Sigma) were added to precipitate the HA-tagged FLCN, and the mixture was incubated overnight at 4 °C. After extensive washing of the beads with NETN buffer, the proteins bound to the beads were eluted in 40 μl of 2× SDS-PAGE sample buffer (120 mM Tris/HCl (pH 6.8), 4% SDS, 20% glycerol, 200 mM DTT, 0.002% bromophenol blue).

For the immunoblotting analyses, immunoprecipitated materials or whole cell extracts prepared by the lysis of cells with 2× SDS-PAGE sample buffer were subjected to SDS-PAGE and electroblotted onto a PVDF membrane (Bio-Rad). Detection was performed using an ECL Plus or Advance Western blotting detection kit (GE Healthcare). The primary antibodies used were: anti-FLAG M2 (Sigma), anti-HA HA-7 (Sigma), anti-FLCN (Protein Tech Group, Inc.), anti-AMPKα (Cell signaling), anti-β-actin (Sigma), and anti-phospho-AMPKα (Thr172) (Cell signaling). Anti-mouse IgG and anti-rabbit IgG conjugated to horseradish peroxidase (GE Healthcare) were used as the secondary antibodies.

2.4. siRNA transfection

Stealth RNAi for the *Mapo1* gene (siMapo1), 5′-CAGAAAGCAGAGGAUGUUCCUAUUA-3′, *Flcn* gene (siFlcn#1), 5′-UUAUUCAGGAUAGUGGGCCCAACUC-3′, (siFlcn#2), 5′-UGGUGACUGACGUACUUAAUAGAGG-3′, and *Ampkα* gene (siAmpkα#1), 5′-UAUCUUAGCGUUCAUCUGGGCAUCC-3′, (siAmpkα#2), 5′-AAGAUGAUAAGCCACUGCAAGCUGG-3′ were purchased from Invitrogen. After culturing 1×10^5 cells in a 6-well plate for one day, the cells were transfected with 20 nM siRNA, using the Lipofectamine RNAiMAX reagent (Invitrogen) according to the manufacturer's protocol. For the control transfection, Stealth RNAi Negative Control Medium GC Duplex (Invitrogen) was used.

2.5. Flow cytometric analysis

For the sub-G_1 population assay, cells were washed with PBS and suspended in 400 μl of PBS containing 0.1% Triton X-100, 25 μg/ml of propidium iodide and 0.1 mg/ml of RNase A. The samples were analyzed using a FACS Calibur flow cytometer (Becton Dickinson), with 10,000 events per determination.

For the mitochondrial membrane depolarization assay, cells were treated with the MitoProbeTM DiOC2(3) Assay Kit (Invitrogen), according to the manufacturer's protocol, and then subjected to analysis using a FACS Calibur flow cytometer.

2.6. Trypan blue exclusion assay

The viability of YT102, KH101 and siRNA-transfected YT102 cells was assayed, based on their trypan blue exclusion. The cells treated with AICA-Ribose were collected 48 h after the drug treatment and were stained with 0.2% trypan blue. The percentage of dead cells was determined as the percentage of trypan blue staining-positive cells. At least 500 cells were counted per experiment.

2.7. Statistics

All *P*-values were generated using two-tailed Student's *t*-tests.

3. Results

3.1. Interaction of MAPO1 with FLCN and AMPK

To confirm that MAPO1 protein interacts with FLCN and AMPK, a co-immunoprecipitation experiment was performed. Whole cell extracts were prepared from mouse YT102 (*Mgmt*$^{-/-}$) cells expressing Flag-tagged MAPO1, and were subjected to immunoprecipitation using an anti-Flag antibody conjugated to agarose beads. The results are shown in Fig. 1A. With whole cell extracts, almost the same intensity of bands for FLCN and AMPKα were detected in both control and Flag-MAPO1-transfected cells. When the materials were immunoprecipitated with the anti-Flag antibody, co-precipitated FLCN and AMPKα were clearly detected, concomitant with the effective precipitation of Flag-MAPO1, whereas no such bands were seen in a sample precipitated from cells treated with the control vector alone.

To evaluate the interaction of FLCN with MAPO1 and AMPK in a reciprocal manner, whole cell extracts prepared from YT102 cells expressing FLAG-tagged MAPO1, with or without HA-tagged FLCN, were applied for immunoprecipitation using an anti-HA antibody (Fig. 1B). When the HA-tagged FLCN was precipitated, as indicated by doublet bands by the immunoblotting analysis, the Flag-tagged MAPO1 and AMPKα were co-precipitated. It is evident, therefore, that MAPO1 interacts with FLCN and AMPK in mouse cells.

3.2. Suppression of the induction of apoptosis in Flcn- and Ampkα-knockdown cells

Since MAPO1 has been identified as an apoptosis-inducing protein, it is plausible that the MAPO1-bound proteins, FLCN and AMPK, might also be involved in apoptosis induction. To examine the possible roles of these proteins, siRNAs specific for the *Flcn* or *Ampkα* genes were introduced into YT102 (*Mgmt*$^{-/-}$) cells. As shown in Fig. 2A and B, two independent siRNAs (siFlcn#1 and #2, and siAmpkα#1 and #2), designed at different sequences of each gene, effectively suppressed the expression of the genes when measured at 48 h after their introduction. The expression level of the *Mapo1* gene in siMapo1-treated cells also decreased to 43% of that in cells that were treated with the control RNA, siCont, as measured by quantitative real time PCR [16]. To monitor the appearance of cells with sub-G_1 DNA content, cells were treated with or without 0.4 mM MNU for 1 h and subjected to a flow cytometric analysis 72 h later. After treatment with MNU, the sub-G_1 cell population increased to more than 20% in the siCont-treated cells (Fig. 2C). Under the same conditions, the degrees of the increases in the cells treated with siRNAs against the *Flcn*, *Ampkα* and *Mapo1* genes were significantly suppressed. These results favor the notion that FLCN and AMPKα, as well as MAPO1, are involved in MNU-induced apoptosis through protein interactions.

3.3. Suppression of the induction of apoptosis by an AMPK inhibitor

The effects of *Ampkα* knockdown on the MNU-induced apoptosis were further examined at multiple time points. The YT102 cells transfected with siCont or siAmpkα#2 were exposed to 0.4 mM MNU for 1 h and then subjected to a flow cytmetric analysis. As shown in Fig. 3A, the sub-G_1 cell population increased gradually, with similar kinetics in cells transfected with either type of siRNA, but the degree of the increase in cells transfected with siAmpkα was significantly lower than that of siCont-transfected cells.

To obtain further evidence supporting the involvement of AMPK in MNU-induced apoptosis, compound C, a specific inhibitor of AMPK, was used to downregulate the function of AMPK. YT102 cells were exposed to 0.4 mM MNU for 1 h, followed by incubation with or without 2 μM of compound C for 72 h, and then cells were subjected to a flow cytometric analysis. As shown in Fig. 3B, the sub-G_1 cell population in compound C-treated cells after MNU treatment significantly decreased in comparison to those not treated with the inhibitor. The inhibitory effects of compound C on AMPK activity were assessed by immunoblotting using an antibody that specifically recognizes a phosphorylated form of AMPKα, since AMPK is activated when the catalytic subunit of AMPKα becomes phosphorylated [27–29]. As shown in Fig. 3C, AMPK appeared to be activated after MNU treatment, while such activation was significantly suppressed by the exposure of cells to compound C. These findings are consistent with the notion that AMPK plays an important role in the induction of apoptosis triggered by MNU.

3.4. MAPO1- and FLCN-dependent activation of AMPK during the induction of apoptosis

To further examine if AMPKα is phosphorylated during the induction of apoptosis, YT102 cells were treated with 1 mM MNU and then collected at 0, 24, 48 and 72 h after treatment. Under these conditions, apoptosis was effectively induced, as was evident by the detection of the mitochondrial membrane depolarization and the caspase-3 activity [16]. The whole cell extracts were prepared, and the phosphorylation levels of AMPKα were assessed by

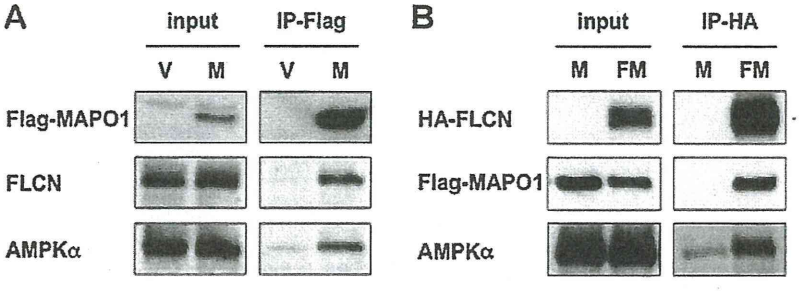

Fig. 1. The association of MAPO1, FLCN and AMPKα proteins. (A) The interaction of MAPO1 with FLCN and AMPKα. YT102 cells were transfected with the pIRES-puro3 vector (termed as V) or pIRES-puro3 containing Flag-tagged *Mapo1* cDNA (termed as M) and harvested after incubation for 24 h. Whole cell extracts (input) were used for immunoprecipitation using anti-Flag M2 antibody beads (IP-Flag). The materials were subjected to SDS-PAGE, transferred to a membrane and immunoblotted using antibodies that recognize the Flag-tag, FLCN and AMPKα. (B) The interaction of FLCN with MAPO1 and AMPKα. YT102 cells were transfected with either pIRES-puro3 containing Flag-tagged *Mapo1* cDNA (termed as M) or pIRE-puro2 carrying HA-tagged *Flcn* cDNA and pIRES-puro3 containing Flag-tagged *Mapo1* cDNA (termed as FM) and were harvested 24 h later. Following immunoprecipitation using anti-HA HA7 antibody beads (IP-HA), an immunoblotting analysis was performed as described in (A) with anti-HA, anti-Flag and anti-AMPKα antibodies.

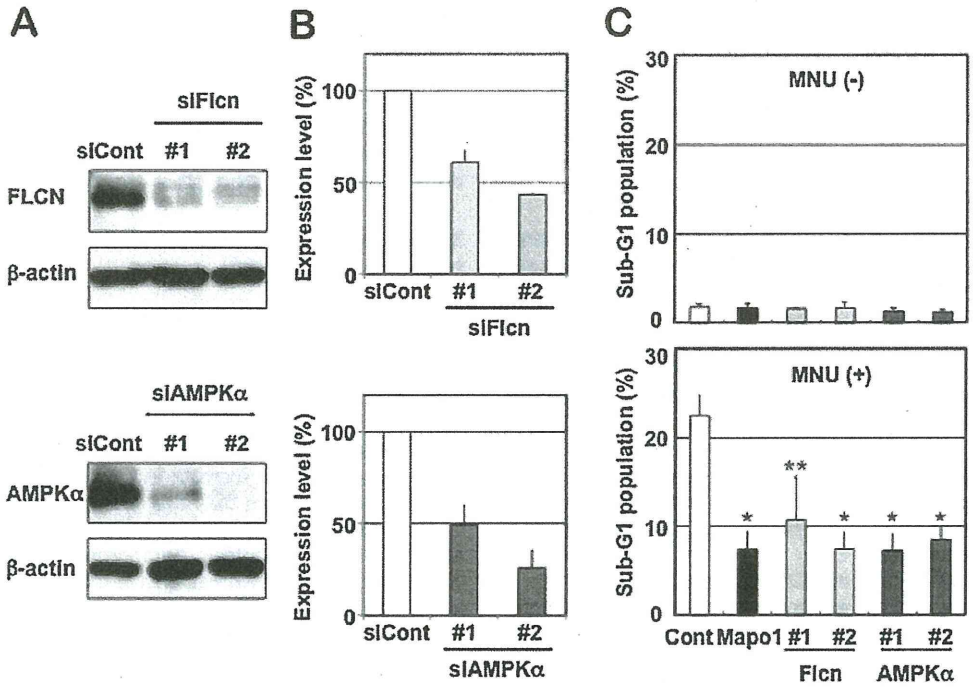

Fig. 2. The suppression of apoptosis by siRNAs targeting the three types of genes. (A) The expression levels of FLCN and AMPKα in cells treated with siRNAs. The whole extracts of YT102 cells transfected with control and two independent siRNAs specific for the corresponding genes were used for the immunoblotting analysis with antibodies specific for FLCN, AMPKα and β-actin (loading control). (B) The relative expression levels of FLCN and AMPKα in the cells treated with siRNAs, as measured by an immunoblotting analysis in (A). (C) The sub-G_1 population of cells transfected with control, *Mapo1*-, *Flcn*- or *Ampkα*-siRNA after MNU treatment. Two days after transfection with siRNA, YT102 cells were treated with or without 0.4 mM MNU for 1 h and then incubated for three days. The cells were harvested and subjected to a flow cytometric analysis. $^*P < 0.01$; $^{**}P < 0.05$ when comparing the sub-G_1 populations in the control and gene-specific siRNA-transfected cells.

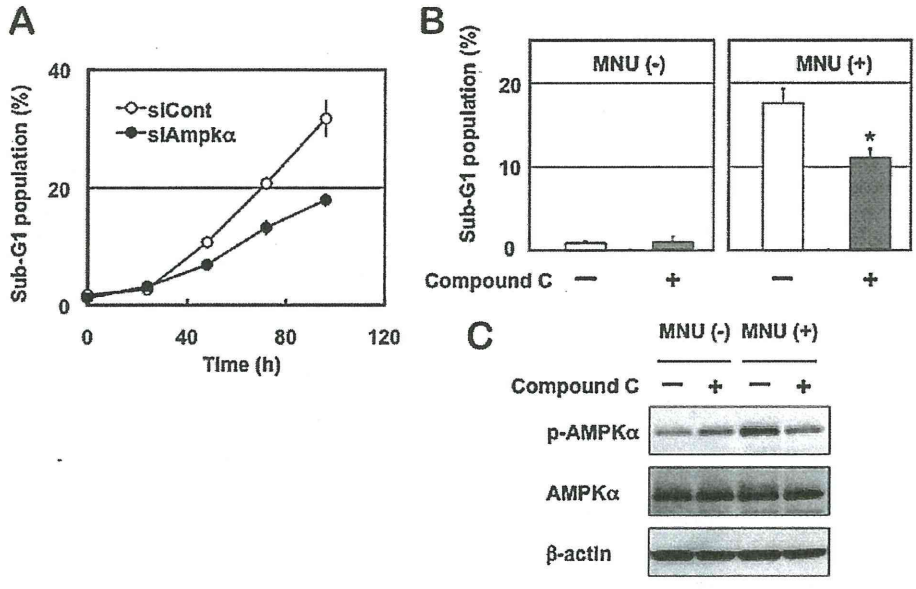

Fig. 3. The involvement of AMPK in MNU-induced apoptosis. (A) The sub-G_1 population of cells transfected with control or *Ampkα* siRNA after MNU treatment. Two days after transfection with siRNA, the YT102 cells were treated with 0.4 mM MNU for 1 h and then harvested at 0, 24, 48, 72 and 96 h after MNU treatment, and subjected to a flow cytometric analysis. The numbers of the cells in the sub-G_1 population were counted and the ratios were plotted. Open circles, siCont-transfected cells; closed circles, siAmpkα-transfected cells. (B) The suppression of apoptosis by an AMPK inhibitor. After treatment with or without 0.4 mM MNU for 1 h, YT102 cells were incubated in medium supplemented with or without 2 μM compound C for three days. The cells were then harvested and subjected to a flow cytometric analysis to monitor the sub-G_1 population of cells. $^*P < 0.01$ when comparing the sub-G_1 populations in compound C-untreated and compound C-treated cells after exposure to MNU. (C) The inhibition of the AMPK activity by compound C. The whole cell extracts from the cells harvested at 48 h after MNU treatment were subjected to an immunoblotting analysis using antibodies that recognize phospho-AMPKα (Thr172), AMPKα and β-actin, respectively.

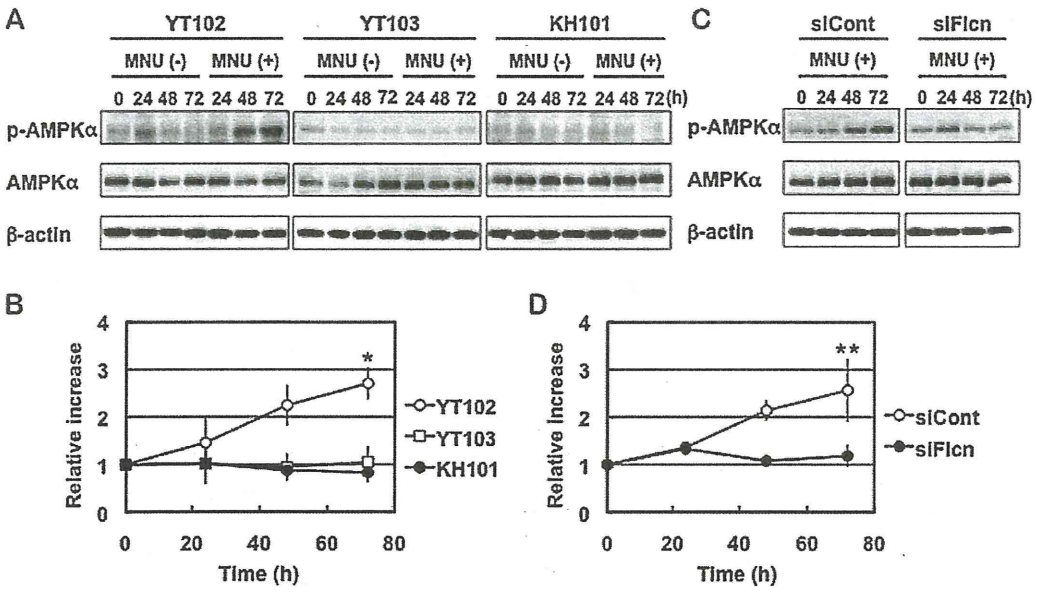

Fig. 4. The activation of AMPK after MNU treatment. (A) The phosphorylation of AMPKα in cells with different genetic backgrounds. Three cell lines, YT102 (*Mgmt*$^{-/-}$), YT103 (*Mgmt*$^{-/-}$ *Mlh1*$^{-/-}$) and KH101 (*Mgmt*$^{-/-}$ *Mapo1*$^{+/-}$), were treated with or without 1 mM MNU for 1 h and then incubated for 0, 24, 48 or 72 h. The whole cell extracts from cells harvested at various times after MNU treatment were subjected to an immunoblotting analysis using antibodies that recognize phospho-AMPKα (Thr172), AMPKα and β-actin, respectively. (B) The relative intensities of the bands for phospho-AMPKα (Thr172) after MNU treatment. Open circles, YT102; open squares, YT103; closed circles, KH101. *$P < 0.01$ when comparing the relative intensities for YT102 cells with those of the YT103 and KH101 cells at 72 h after exposure to MNU. (C) Activation of AMPK in cells transfected with *Flcn*-siRNA. Two days after transfection with control or *Flcn*-siRNA, the YT102 cells were treated with or without 1 mM MNU for 1 h. The analysis was performed as described above. (D) The relative intensities of bands for phospho-AMPKα (Thr172) after MNU treatment. Open circles, siCont-transfected cells; closed circles, siFlcn-transfected cells. **$P < 0.05$ when comparing the relative intensities of the control and *Flcn*-specific siRNA-transfected cells at 72 h after exposure to MNU.

an immunoblotting analysis. As shown in Fig. 4A and B, the levels of phosphorylation of AMPKα increased gradually and reached about 2.7-folds at 72 h after MNU treatment, whereas no such increase was observed in cells not expose to MNU. The amounts of the AMPKα protein were almost constant under these situations. In YT103 (*Mgmt*$^{-/-}$ *Mlh1*$^{-/-}$) cells, which are unable to induce apoptosis due to their lack of the *Mlh1* gene, the increase of phosphorylated forms of AMPKα was hardly detectable, even after MNU treatment. These results indicate that AMPK is activated during the course of the induction of apoptosis, triggered in a mismatch repair protein-dependent manner. To evaluate the effects of *Mapo1* mutation on the activation of AMPK, we used KH101 (*Mgmt*$^{-/-}$ *Mapo1*$^{+/-}$) cells, which carry an insertional mutation in one of the alleles of the *Mapo1* gene and exhibit haploinsufficiency for the induction of apoptosis triggered by MNU treatment [16]. Similar to the results described above, no increase in the band corresponding to phosphorylated AMPKα was detected even after treatment with MNU (Fig. 4A and B). Since MAPO1 interacts with FLCN (Fig. 1), it was supposed that FLCN might also play a role in the activation of AMPK during the course of apoptosis. To examine this possibility, YT102 (*Mgmt*$^{-/-}$) cells were transfected with siRNA targeting the *Flcn* gene (siFlcn#2), and then were exposed to 1 mM MNU for 1 h. The immunoblotting analyses of these samples collected after incubation for 0, 24, 48 and 72 h revealed that phosphorylation of AMPKα, which occurred gradually in siCont-transfected cells, did not take place in the siFlcn-transfected ones (Fig. 4C and D). These results indicate that the activation of AMPK, which occurs during the course of MNU-induced apoptosis, is dependent on the functions of both FLCN and MAPO1.

3.5. Induction of apoptosis through activation of AMPK

To confirm the importance of the activation of AMPK for the induction of apoptosis, AICA-Ribose (AICAR), a specific activator of AMPK, was applied to YT102 cells. After treatment with a low dose (0.2 mM) of AICAR for 48 h, the viabilities of cells were analyzed, based on the trypan blue exclusion assay. As shown in Fig. 5A, there was a significant increase of trypan blue staining-positive cells after treatment with AICAR in the YT102 (*Mgmt*$^{-/-}$ *Mapo1*$^{+/+}$) cells, whereas no such increase was observed in the *Mapo1*-defective KH101 (*Mgmt*$^{-/-}$ *Mapo1*$^{+/-}$) cells even after the same treatment. To determine if the increase in dead cells was related to the induction of apoptosis, the cells were subjected to an assay for mitochondrial membrane depolarization, which is known to occur during the process of apoptosis. The results are shown in Fig. 5B and C. The depolarization of the mitochondrial membrane was induced after treatment with AICAR in YT102 cells, but not in *Mapo1*-defective KH101 cells. The results indicate that the function of MAPO1 is necessary for AICAR-induced apoptosis. An immunoblotting experiment, the results of which are shown in Fig. 5D, revealed that the AICAR-treatment induced phosphorylation of AMPKα to the similar level to that when treated with MNU, however, such an induction did not occur in the *Mapo1*-defective KH101 cells. These results suggest that the activation of AMPK is important for the induction of apoptosis, and that a normal level of MAPO1 is necessary for the activation of AMPK.

We next examined if FLCN, which interacts with MAPO1, is also required for the AICAR-induced cell death. For this study, we applied AICAR to YT102 cells whose FLCN function was knocked down by siRNA (siFlcn#2). As shown in Fig. 6A–C, the degree of AICAR-induced cell death, which was accompanied by the depolarization of the mitochondrial membrane, was significantly lower in siFlcn-transfected cells as compared to that in siCont-transfected ones. Furthermore, the AICAR-induced AMPKα phosphorylation was almost completely blocked in siFlcn-transfected cells (Fig. 6D). Therefore, these results suggest that FLCN is required for AMPK activation, as well as the cell death induced by the treatment with AICAR.

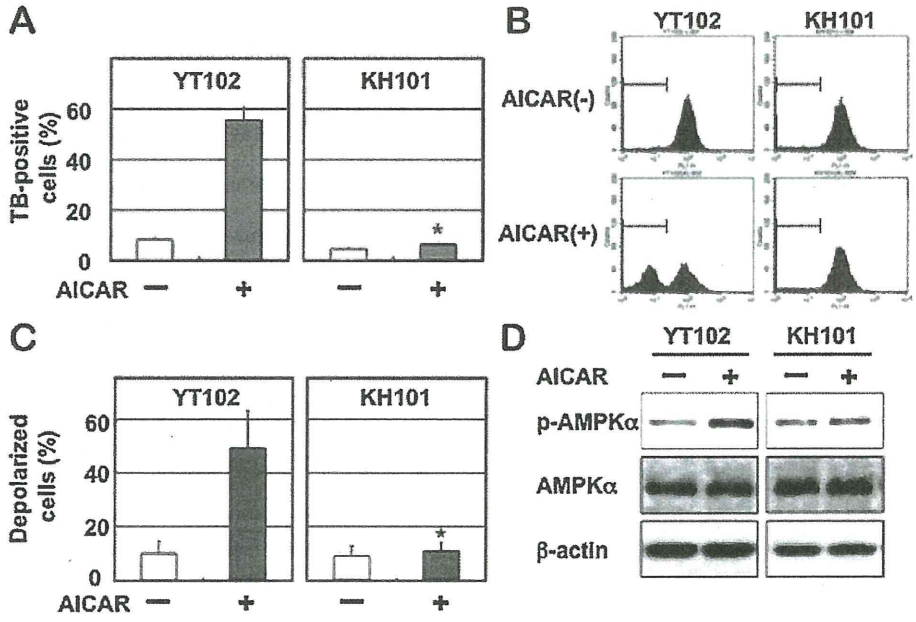

Fig. 5. MAPO1-dependent cell death induced by an AMPK activator. *Mapo1*-proficient YT102 and *Mapo1*-defective KH101 cells were incubated in a medium supplemented with or without 0.2 mM AICAR for two days and then harvested. (A) The viabilities of the cells. The numbers of cells stained with trypan blue (TB) were counted and the ratios are shown. *$P < 0.01$ when comparing the TB-positive YT102 and KH101 cells after exposure to AICAR. (B) Depolarization of the mitochondrial membrane. The cells were evaluated by a mitochondrial membrane depolarization assay, and representative patterns of the assay are shown. The populations of depolarized cells were gated by bars. (C) The levels of mitochondrial membrane depolarization. The mean values obtained from three independent experiments in (B) and the standard deviations (bars) are presented. *$P < 0.01$ when comparing the depolarized cells in YT102 and KH101 cells after exposure to AICAR. (D) Activation of AMPK after treatment with AICAR. The whole cell extracts prepared from cells, treated with or without AICAR, were subjected to an immunoblotting analysis using antibodies specific for phospho-AMPKα (Thr172), AMPKα and β-actin, respectively.

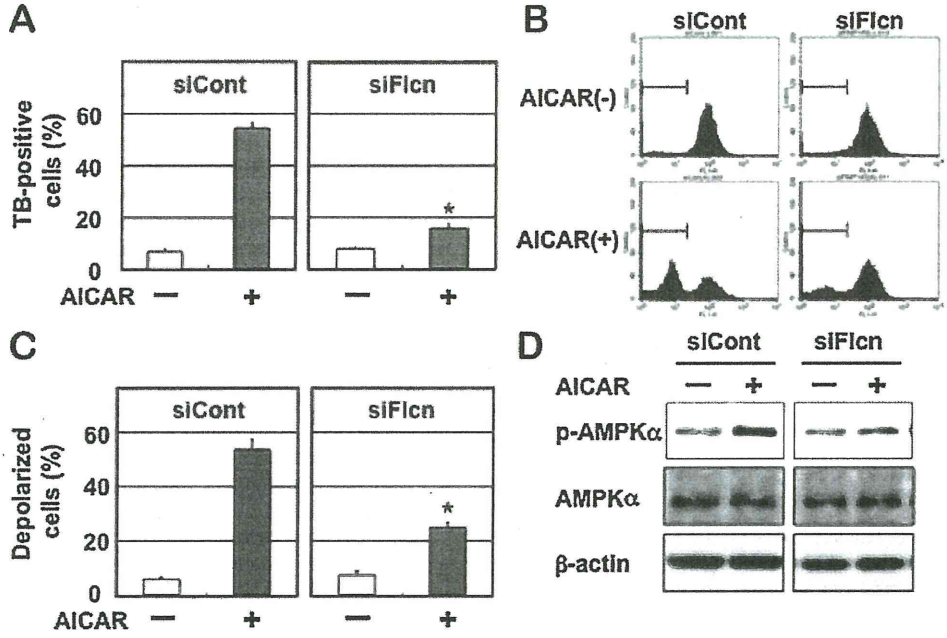

Fig. 6. FLCN-dependent cell death induced by an AMPK activator. YT102 cells transfected with control- or *Flcn*-siRNA were cultured with or without 0.2 mM AICAR for two days and then harvested. (A) The viabilities of the cells. The numbers of cells stained with trypan blue (TB) were counted and the ratios are shown. *$P < 0.01$ when comparing the TB-positive siCont-transfected and siFlcn-transfected cells after exposure to AICAR. (B) Depolarization of the mitochondrial membrane. The cells were evaluated by a mitochondrial membrane depolarization assay, and representative patterns of the assay are shown. The populations of depolarized cells were gated by bars. (C) The levels of mitochondrial membrane depolarization. The mean values obtained from three independent experiments in (B) and the standard deviations (bars) are presented. *$P < 0.01$ when comparing the depolarized cells in siCont-transfected and siFlcn-transfected cells after exposure to AICAR. (D) Activation of AMPK after treatment with AICAR. The whole cell extracts prepared from AICAR-treated or -untreated cells, were subjected to an immunoblotting analysis using antibodies specific for phospho-AMPKα (Thr172), AMPKα and β-actin, respectively.

4. Discussion

MAPO1 was identified as one of the protein elements functioning at a certain step following the induction of apoptosis [16]. In *Mapo1*-defective cells, mitochondrial membrane depolarization and caspase-3 activation were not observed even after exposure to MNU, although the cells retain the ability for mismatch repair protein-dependent DNA damage detection and signaling. Subsequent studies have revealed that MAPO1 is identical to FNIP2 and FNIPL, reported by Hasumi et al. [23] and Takagi et al. [24], respectively. This protein is bound to folliculin, encoded by the *FLCN* tumor suppressor gene, and AMP-activated protein kinase (AMPK). To analyze the possible roles of folliculin and AMPK in the induction of apoptosis, we introduced siRNAs specific for the *Flcn* or *Ampkα* gene and then treated the cells with MNU. The flow cytometric analyses performed to measure the sub-G_1 population of cells revealed that folliculin and AMPK, as well as MAPO1, were involved in MNU-induced apoptosis. Taken together, these data suggest that MAPO1 forms a protein complex(es) with folliculin and AMPK, and plays a role in a signal transduction pathway of apoptosis.

It is known that AMPK is one of the signaling kinases that negatively regulates cell growth and proliferation and is phosphorylated itself under conditions of energetic stress [26–29]. Several recent papers have observed the pro-apoptotic potential of activated AMPK [30–33]. In this report, we found a gradual increase in the levels of AMPK phosphorylation in *Mapo1*-proficient cells after MNU treatment, implying a possible involvement of the activation of AMPK in the MNU-induced apoptosis pathway. In *Mapo1*-deficient cells, AMPK activation in this manner was hardly detectable, even after the treatment with MNU. Furthermore, the treatment of cells with AICAR, a specific activator of AMPK, resulted in AMPKα phosphorylation and mitochondrial membrane depolarization in a *Mapo1*-dependent manner. These findings extended onto the case of *Flcn*-knockdown cells. Taken together, it is likely that MAPO1 and FLCN positively regulate the activation of AMPK through their mutual interaction in the apoptotic signaling pathway, triggered by an alkylating agent. MAPO1 and FLCN proteins have been reported to undergo some modifications in cells [17,24]. The treatment with an alkylating agent might affect the modified states of these proteins, and might cause the activation of the protein complex, thus leading to AMPK activation. Another folliculin-interacting protein, FNIP1, which is homologous to MAPO1, is also capable of binding to AMPK [17]. The activation of AMPK might therefore be regulated in more complex ways under the balance of MAPO1 and FNIP1 activities.

Another important problem which remains to be solved is how the AMPK–MAPO1–FLCN complex is activated by the signal delivered from the mismatch repair protein complex, which itself is activated through the interaction with DNA carrying base mismatches. The signal may be delivered by direct physical contact between the two complexes or through the involvement of other protein factors. The protein linking analyses, aided by mass spectrometry, have been performed, but no evidence to show the physical association of the two complexes was obtained (unpublished results). It seems likely, therefore, that some other protein factor(s) might be involved in the signal transduction process. To identify such factors, it would be relevant to extend this approach using retrovirus-mediated gene-trap mutagenesis studies.

Germline mutations in the *FLCN* gene have been identified in patients with Birt-Hogg-Dubé (BHD) syndrome, which is an autosomal dominant disorder characterized by hamartomas of skin follicles, spontaneous pneumothorax, and renal tumors [20–22]. Furthermore, *BHD* heterozygous knockout mice were revealed to develop kidney cysts and tumors as they aged, while *BHD* homozygous null mice displayed early embryonic lethality [34,35]. The recent findings, including this report, strongly suggest that folliculin has physical and/or functional interactions with the AMPK-mTOR signaling pathway [17,34,36]. Mutations in several other tumor suppressor genes, such as *LKB1*, *TSC1* and *TSC2* [29,37], have also been shown to lead to dysregulation of AMPK-mTOR signaling and to the development of other hamartomatous syndromes. Our present findings that folliculin is involved in the induction of apoptosis might shed some light on the physiological roles of *BHD/FLCN* and other related tumor suppressor genes. We are currently establishing *Mapo1* knockout mice to analyze the possible roles of the gene in the suppression of tumor predisposition resulting from environmental stresses.

Conflict of interest statement

The authors declare that there are no conflicts of interests.

Acknowledgments

We thank Drs. H. Hayakawa and Y. Takagi (Fukuoka Dental College, Japan) for helpful discussion. This work was supported by grants (including a Frontier Research Grant) from the Ministry of Education, Culture, Sports, Science and Technology of Japan, and from the Ministry of Health, Labor and Welfare of Japan.

References

[1] D.T. Beranek, Distribution of methyl and ethyl adducts following alkylation with monofunctional alkylating agents, Mutat. Res. 231 (1990) 11–30.
[2] C. Coulondre, J.H. Miller, Genetic studies of the lac repressor. IV. Mutagenic specificity in the lacI gene of *Escherichia coli*, J. Mol. Biol. 117 (1977) 577–606.
[3] T. Ito, T. Nakamura, H. Maki, M. Sekiguchi, Roles of transcription and repair in alkylation mutagenesis, Mutat. Res. 314 (1994) 273–285.
[4] B. Demple, A. Jacobsson, M. Olsson, P. Robins, T. Lindahl, Repair of alkylated DNA in *Escherichia coli*. Physical properties of O6-methylguanine–DNA methyltransferase, J. Biol. Chem. 257 (1982) 13776–13780.
[5] H. Kawate, K. Ihara, K. Kohda, K. Sakumi, M. Sekiguchi, Mouse methyltransferase for repair of O6-methylguanine and O4-methylthymine in DNA, Carcinogenesis 16 (1995) 1595–1602.
[6] P. Branch, G. Aquilina, M. Bignami, P. Karran, Defective mismatch binding and a mutator phenotype in cells tolerant to DNA damage, Nature 362 (1993) 652–654.
[7] M. Hidaka, Y. Takagi, T.Y. Takano, M. Sekiguchi, PCNA-MutSalpha-mediated binding of MutLalpha to replicative DNA with mismatched bases to induce apoptosis in human cells, Nucleic Acids Res. 33 (2005) 5703–5712.
[8] A. Kat, W.G. Thilly, W.H. Fang, M.J. Longley, G.M. Li, P. Modrich, An alkylation-tolerant, mutator human cell line is deficient in strand-specific mismatch repair, Proc. Natl. Acad. Sci. U.S.A. 90 (1993) 6424–6428.
[9] B.J. Glassner, G. Weeda, J.M. Allan, J.L. Broekhof, N.H. Carls, I. Donker, B.P. Engelward, R.J. Hampson, R. Hersmus, M.J. Hickman, R.B. Roth, H.B. Warren, M.M. Wu, J.H. Hoeijmakers, L.D. Samson, DNA repair methyltransferase (Mgmt) knockout mice are sensitive to the lethal effects of chemotherapeutic alkylating agents, Mutagenesis 14 (1999) 339–347.
[10] K. Sakumi, A. Shiraishi, S. Shimizu, T. Tsuzuki, T. Ishikawa, M. Sekiguchi, Methylnitrosourea-induced tumorigenesis in MGMT gene knockout mice, Cancer Res. 57 (1997) 2415–2418.
[11] A. Shiraishi, K. Sakumi, M. Sekiguchi, Increased susceptibility to chemotherapeutic alkylating agents of mice deficient in DNA repair methyltransferase, Carcinogenesis 21 (2000) 1879–1883.
[12] T. Tsuzuki, K. Sakumi, A. Shiraishi, H. Kawate, H. Igarashi, T. Iwakuma, Y. Tominaga, S. Zhang, S. Shimizu, T. Ishikawa, et al., Targeted disruption of the DNA repair methyltransferase gene renders mice hypersensitive to alkylating agent, Carcinogenesis 17 (1996) 1215–1220.
[13] H. Kawate, K. Sakumi, T. Tsuzuki, Y. Nakatsuru, T. Ishikawa, S. Takahashi, H. Takano, T. Noda, M. Sekiguchi, Separation of killing and tumorigenic effects of an alkylating agent in mice defective in two of the DNA repair genes, Proc. Natl. Acad. Sci. U.S.A. 95 (1998) 5116–5120.
[14] Y. Takagi, M. Takahashi, M. Sanada, R. Ito, M. Yamaizumi, M. Sekiguchi, Roles of MGMT and MLH1 proteins in alkylation-induced apoptosis and mutagenesis, DNA Repair (Amst.) 2 (2003) 1135–1146.
[15] K. Ochs, B. Kaina, Apoptosis induced by DNA damage O6-methylguanine is Bcl-2 and caspase-9/3 regulated and Fas/Caspase-8 independent, Cancer Res. 60 (2000) 5815–5824.
[16] K. Komori, Y. Takagi, M. Sanada, T.H. Lim, Y. Nakatsu, T. Tsuzuki, M. Sekiguchi, M. Hidaka, A novel protein, MAPO1, that functions in apoptosis triggered by O6-methylguanine mispair in DNA, Oncogene 28 (2009) 1142–1150.
[17] M. Baba, S.B. Hong, N. Sharma, M.B. Warren, M.L. Nickerson, A. Iwamatsu, D. Esposito, W.K. Gillette, R.F. Hopkins 3rd, J.L. Hartley, M. Furihata, S. Oishi, W. Zhen, T.R. Burke, W.M. Linehan Jr., L.S. Schmidt, B. Zbar, Folliculin encoded

by the BHD gene interacts with a binding protein, FNIP1, and AMPK and is involved in AMPK and mTOR signaling, Proc. Natl. Acad. Sci. U.S.A. 103 (2006) 15552–15557.
[18] M.L. Nickerson, M.B. Warren, J.R. Toro, V. Matrosova, G. Glenn, M.L. Turner, P. Duray, M. Merino, P. Choyke, C.P. Pavlovich, N. Sharma, M. Walther, D. Munroe, R. Hill, E. Maher, C. Greenberg, M.I. Lerman, W.M. Linehan, B. Zbar, L.S. Schmidt, Mutations in a novel gene lead to kidney tumors, lung wall defects, and benign tumors of the hair follicle in patients with the Birt-Hogg-Dube syndrome, Cancer Cell 2 (2002) 157–164.
[19] C.D. Vocke, Y. Yang, C.P. Pavlovich, L.S. Schmidt, M.L. Nickerson, C.A. Torres-Cabala, M.J. Merino, M.M. Walther, B. Zbar, W.M. Linehan, High frequency of somatic frameshift BHD gene mutations in Birt-Hogg-Dube-associated renal tumors, J. Natl. Cancer Inst. 97 (2005) 931–935.
[20] A.R. Birt, G.R. Hogg, W.J. Dube, Hereditary multiple fibrofolliculomas with trichodiscomas and acrochordons, Arch. Dermatol. 113 (1977) 1674–1677.
[21] J.R. Toro, G. Glenn, P. Duray, T. Darling, G. Weirich, B. Zbar, M. Linehan, M.L. Turner, Birt-Hogg-Dube syndrome: a novel marker of kidney neoplasia, Arch. Dermatol. 135 (1999) 1195–1202.
[22] B. Zbar, W.G. Alvord, G. Glenn, M. Turner, C.P. Pavlovich, L. Schmidt, M. Walther, P. Choyke, G. Weirich, S.M. Hewitt, P. Duray, F. Gabril, C. Greenberg, M.J. Merino, J. Toro, W.M. Linehan, Risk of renal and colonic neoplasms and spontaneous pneumothorax in the Birt-Hogg-Dube syndrome, Cancer Epidemiol. Biomarkers Prev. 11 (2002) 393–400.
[23] H. Hasumi, M. Baba, S.B. Hong, Y. Hasumi, Y. Huang, M. Yao, V.A. Valera, W.M. Linehan, L.S. Schmidt, Identification and characterization of a novel folliculin-interacting protein FNIP2, Gene 415 (2008) 60–67.
[24] Y. Takagi, T. Kobayashi, M. Shiono, L. Wang, X. Piao, G. Sun, D. Zhang, M. Abe, Y. Hagiwara, K. Takahashi, O. Hino, Interaction of folliculin (Birt-Hogg-Dube gene product) with a novel Fnip1-like (FnipL/Fnip2) protein, Oncogene 27 (2008) 5339–5347.
[25] D. Carling, The AMP-activated protein kinase cascade – a unifying system for energy control, Trends Biochem. Sci. 29 (2004) 18–24.
[26] D.G. Hardie, The AMP-activated protein kinase pathway – new players upstream and downstream, J. Cell Sci. 117 (2004) 5479–5487.
[27] S.A. Hawley, M. Davison, A. Woods, S.P. Davies, R.K. Beri, D. Carling, D.G. Hardie, Characterization of the AMP-activated protein kinase from rat liver and identification of threonine 172 as the major site at which it phosphorylates AMP-activated protein kinase, J. Biol. Chem. 271 (1996) 27879–27887.
[28] J.M. Lizcano, O. Goransson, R. Toth, M. Deak, N.A. Morrice, J. Boudeau, S.A. Hawley, L. Udd, T.P. Makela, D.G. Hardie, D.R. Alessi, LKB1 is a master kinase that activates 13 kinases of the AMPK subfamily, including MARK/PAR-1, EMBO J. 23 (2004) 833–843.
[29] R.J. Shaw, M. Kosmatka, N. Bardeesy, R.L. Hurley, L.A. Witters, R.A. DePinho, L.C. Cantley, The tumor suppressor LKB1 kinase directly activates AMP-activated kinase and regulates apoptosis in response to energy stress, Proc. Natl. Acad. Sci. U.S.A. 101 (2004) 3329–3335.
[30] C. Cao, S. Lu, R. Kivlin, B. Wallin, E. Card, A. Bagdasarian, T. Tamakloe, W.M. Chu, K.L. Guan, Y. Wan, AMP-activated protein kinase contributes to UV- and H2O2-induced apoptosis in human skin keratinocytes, J. Biol. Chem. 283 (2008) 28897–28908.
[31] R.G. Jones, D.R. Plas, S. Kubek, M. Buzzai, J. Mu, Y. Xu, M.J. Birnbaum, C.B. Thompson, AMP-activated protein kinase induces a p53-dependent metabolic checkpoint, Mol. Cell 18 (2005) 283–293.
[32] R. Okoshi, T. Ozaki, H. Yamamoto, K. Ando, N. Koida, S. Ono, T. Koda, T. Kamijo, A. Nakagawara, H. Kizaki, Activation of AMP-activated protein kinase induces p53-dependent apoptotic cell death in response to energetic stress, J. Biol. Chem. 283 (2008) 3979–3987.
[33] W.B. Zhang, Z. Wang, F. Shu, Y.H. Jin, H.Y. Liu, Q.J. Wang, Y. Yang, Activation of AMP-activated protein kinase by temozolomide contributes to apoptosis in glioblastoma cells via p53 activation and mTORC1 inhibition, J. Biol. Chem. 285 (2010) 40461–40471.
[34] T.R. Hartman, E. Nicolas, A. Klein-Szanto, T. Al-Saleem, T.P. Cash, M.C. Simon, E.P. Henske, The role of the Birt-Hogg-Dube protein in mTOR activation and renal tumorigenesis, Oncogene 28 (2009) 1594–1604.
[35] Y. Hasumi, M. Baba, R. Ajima, H. Hasumi, V.A. Valera, M.E. Klein, D.C. Haines, M.J. Merino, S.B. Hong, T.P. Yamaguchi, L.S. Schmidt, W.M. Linehan, Homozygous loss of BHD causes early embryonic lethality and kidney tumor development with activation of mTORC1 and mTORC2, Proc. Natl. Acad. Sci. U.S.A. 106 (2009) 18722–18727.
[36] X. Piao, T. Kobayashi, L. Wang, M. Shiono, Y. Takagi, G. Sun, M. Abe, Y. Hagiwara, D. Zhang, K. Okimoto, M. Kouchi, I. Matsumoto, O. Hino, Regulation of folliculin (the BHD gene product) phosphorylation by Tsc2-mTOR pathway, Biochem. Biophys. Res. Commun. 389 (2009) 16–21.
[37] K. Inoki, M.N. Corradetti, K.L. Guan, Dysregulation of the TSC-mTOR pathway in human disease, Nat. Genet. 37 (2005) 19–24.

GASTROENTEROLOGY 2011;140:1556–1563

JNK Signaling Promotes Intestinal Tumorigenesis Through Activation of mTOR Complex 1 in *Apc*$^{\Delta 716}$ Mice

TERUAKI FUJISHITA, MASAHIRO AOKI, and MAKOTO M. TAKETO

Department of Pharmacology, Graduate School of Medicine, Kyoto University, Yoshida-Konoé-Cho, Sakyo-Ku, Kyoto, Japan

See editorial on page 1387.

BACKGROUND & AIMS: Signaling by the mammalian target of rapamycin complex 1 (mTORC1) has been implicated in various human cancers. mTORC1 signaling is activated in intestinal tumors of adenomatous polyposis coli (*Apc*$^{\Delta 716}$) mice, a model of familial adenomatous polyposis; in these mice, the mTORC1 inhibitor RAD001 can block tumor formation. However, the precise mechanism of mTORC1 signaling in intestinal tumors is not clear. We investigated whether c-Jun-NH_2 terminal kinase (JNK) is involved in the mTORC1 activation. **METHODS:** We investigated the effects of an inhibitor and an activator of JNK, as well as small interfering RNA against JNK, on mTORC1 in *Apc*$^{\Delta 716}$ mice and colon cancer cell lines. We also determined the role of JNK in mTORC1 signaling using in vitro kinase assays. **RESULTS:** JNK was activated in intestinal polyps of *Apc*$^{\Delta 716}$ mice; the JNK inhibitor SP600125 significantly suppressed tumor formation. In colorectal cancer cell lines, the JNK activator anisomycin activated mTORC1, whereas SP600125 or small interfering RNAs against JNK suppressed signaling. Importantly, JNK stimulated the mTORC1 kinase activity in vitro, through direct phosphorylation of Raptor at serine 863. **CONCLUSIONS: JNK is required for activation of mTORC1 in intestinal tumor cells. JNK inhibitors might be developed as therapeutics or to prevent development of intestinal tumors.**

Keywords: mTORC1; JNK; Intestinal Tumor.

BASIC—ALIMENTARY TRACT

Mammalian target of rapamycin (mTOR) is a serine/threonine kinase that can form 2 complexes with distinct functions: mTORC1 and mTORC2.[1] Although mTORC1 is composed of mTOR, Raptor, and mLST8 (and PRAS40), mTORC2 consists of mTOR, Rictor, mLST8, mSin1, and Protor.[2] It is known that mTORC1 phosphorylates p70 s6 kinase (S6K) and eukaryotic initiation factor 4E-binding protein 1 (4EBP1), and thereby enhances translation of subsets of messenger RNAs (mRNAs). Activation of mTORC1 signaling thus promotes protein synthesis and cell growth. On the other hand, mTORC2 can phosphorylate Akt and serum/glucocorticoid regulated kinase, and promote actin organization as well.[2]

Although prototypic mTORC1 inhibitor sirolimus (rapamycin) has been used as an immunosuppressive agent to prevent rejection of transplanted organs, its derivatives have been tested for cancer therapy because of their growth-inhibitory effects. Namely, everolimus (RAD001) and temsirolimus (CCI-779) have been approved by the Food and Drug Administration to treat advanced renal cell calcinoma,[3,4] and clinical trials for mTORC1 inhibitors are ongoing for several types of cancer.[5]

Colorectal cancer is one of the leading causes of cancer deaths. We previously showed that RAD001 suppressed intestinal tumorigenesis in adenomatous polyposis coli (*Apc*$^{\Delta 716}$) mice, and extended their survival significantly, suggesting that mTORC1 inhibition could be a useful colon cancer therapy.[6] Although the study showed that Wnt/β-catenin signaling contributed to mTORC1 activation by increasing the mTOR protein level, it was unclear whether Wnt/β-catenin signaling was sufficient for mTORC1 activation in the intestinal polyps of *Apc*$^{\Delta 716}$ mice.

The c-Jun N-terminal kinase (JNK) is a serine/threonine kinase that affects proliferation, differentiation, survival, and migration.[7] The JNK signaling is activated in human colon cancer tissues,[8] and has been implicated in some other types of cancer as well. Namely, *Jnk1* knockout reduced hepatocellular carcinogenesis induced by diethylnitrosamine,[9] as well as gastric cancer formation induced by N-methyl-N-nitrosourea.[10] Furthermore, the number and size of polyps in *Apc*^{min} mouse intestines were reduced by introduction of a c-Jun mutation carrying alanine substitutions at the JNK phosphorylation sites.[11] Interestingly, some of the phenotypes of *Jnk1* knockout mice are similar to those of mutants in S6K, an mTORC1 substrate. For example, mutant mice for either gene show decreased body weight and reduced levels of

Abbreviations used in this paper: Apc, adenomatous polyposis coli; mTOR, mammalian target of rapamycin; JNK, c-Jun-NH_2 terminal kinase; shRNA, short hairpin RNA; siRNA, small interfering RNA; WT, wild-type.

0016-5085/$36.00
doi:10.1053/j.gastro.2011.02.007

circulating insulin.[12-14] Here we show that activation of JNK signaling induces mTORC1 signaling, and that inhibition of JNK signaling reduces intestinal tumorigenesis. We also show that JNK can directly activate mTORC1 through phosphorylation of Raptor.

Materials and Methods

Animals and Drug Treatments

The construction of $Apc^{\Delta 716}$ knockout mice was described previously.[15] Male and female $Apc^{\Delta 716}$ mice at 8 weeks of age were gavaged with SP600125 (50 mg/kg/day) (Sigma Chemical Co, St. Louis, MO) or the vehicle (0.5% hydroxyethyl cellulose) for 4 weeks. RAD001 (everolimus) was provided by Novartis Institutes for BioMedical Research (Basel, Switzerland). A total of 10 mg/kg/day of RAD001 was administered for 2 weeks as microemulsion containing 2% (wt/wt) RAD001 diluted in distilled deionized water by oral gavage. All animal experiments were performed according to the protocols approved by the Animal Care and Use Committee of Kyoto University.

Histologic Analysis and Immunohistochemistry

Tissues were fixed in 10% formalin-phosphate-buffered saline (PBS) for staining p-c-Jun or in 4% paraformaldehyde–PBS for staining p-S6, β-catenin, and proliferin. Paraffin-embedded samples were sectioned at 4-μm thickness and stained with H&E or subjected to immunohistochemistry. Sections were stained with antibodies against β-catenin (Sigma), p-S6, p-c-Jun (Cell Signaling Technology, Danvers, MA), or proliferin (R&D Systems, Minneapolis, MN), with prior antigen retrieval by microwave in sodium citrate buffer (pH 6.0). After the incubation with primary antibodies, sections were incubated with biotinylated secondary antibodies (Vector Laboratories, Burlingame, CA). The peroxidase activity was detected with Vectorstain Elite kit (Vector Laboratories) and DAB Substrate kit (Vector Laboratories).

Polyp Scoring

Intestinal polyps were counted as described previously.[15] Briefly, the small and large intestines were excised, washed with ice-cold PBS, and opened longitudinally. After fixation with 4% paraformaldehyde–PBS, the number and size of polyps were scored under a dissection microscope.

Cell Cultures and Transfection

We obtained human colon cancer cell lines SW480 and HT29 from M. Tsujii (Osaka University, Osaka, Japan). RKO cells were purchased from American Type Culture Collection. Cells were cultured in Dulbecco's modified Eagle medium supplemented with 10% fetal bovine serum (Biowest, Nuaille, France). For starvation, the cells were cultured in serum-free Dulbecco's modified Eagle medium or in Dulbecco's PBS containing 45 mmol/L glucose. SP600125 (Sigma) and anisomycin (Sigma) were dissolved in dimethyl sulfoxide, and then used to treat the cells at concentrations of 50 μmol/L and 1 μg/mL, respectively. Expression vectors were transfected using Lipofectamine 2000 (Invitrogen, Carlsbad, CA). Transfection with siRNA was performed using Lipofectamine 2000 (Invitrogen), adjusting the final RNA concentration to 40 nmol/L. The small interfering RNAs (siRNAs) were designed to target human *APC* (Verma et al[16]; Dharmacon, Lafayette, CO) and c-Jun (5′-GGAAGCUGGAGAGAAUCGCdTdT-3′; Hayashi Kasei, Osaka, Japan). Scramble RNA was used as a control (Hokkaido System Science, Sapporo, Japan).

Western Blot Analysis

Western blot analysis was performed as described previously.[6] Whole lysates of the intestinal polyps were prepared from 2–3 polyps per sample. The lysates were applied to sodium dodecyl sulfate-polyacrylamide gel electrophoresis, transferred to a polyvinylidene fluoride microporous membrane (Millipore, Billerica, MA), and immunoblotted with antibodies for cyclin E, c-myc tag (Santa Cruz, Santa Cruz, CA), β-catenin, β-actin (Sigma), p-JNK1/2, p-c-Jun, p-S6, S6, p-S6 kinase, S6 kinase, p-4EBP1, 4EBP1, p-Akt (Cell Signaling Technology), proliferin (R&D Systems), osteopontin (IBL, Fujioka, Japan), MMP7 (Merck, Darmstadt, Germany), c-Myc (Millipore), or His-tag (MBL, Nagoya, Japan). Immuno-specific bands were detected by chemiluminescence using Immobilon Western Chemiluminescent Horseradish-Peroxidase Substrate (Millipore).

Reverse-Transcription Polymerase Chain Reaction Analysis

Total RNA from cultured cells or mouse tissues was extracted using TRI Reagent (Sigma), according to the manufacturer's protocol. Each RNA sample (4 μg) was reverse-transcribed and subjected to polymerase chain reaction under the following conditions: cyclin E: denaturation at 94°C for 45 seconds, annealing at 60°C for 45 seconds, and extension at 72°C for 1 minute, for 28 cycles; proliferin and osteopontin: denaturation at 94°C for 30 seconds, annealing at 55°C for 45 seconds, and extension at 72°C for 1 minute, for 28 cycles. The primers for human cyclin E were as follows: 5′-AATCGACAGGACGGCGAGGGAC- 3′ (forward) and 5′-GGCAGTCAACATCCAGGACACA-3′ (reverse). The primers for mouse proliferin were as follows: 5′-TGTGTGCAATGAGGAATGGT-3′ (forward) and 5′-AACCAGGCAGGGTTCTTCTT-3′ (reverse). The primers for mouse osteopontin were as follows: 5′-AAGCTTCCATGGGAATTGGAGTGATTTGCTTTTGCCTC-3′ (forward) and 5′-GGATCCTTAATTGACCTCAGAAGATGCACTATCTAA-3′ (reverse). The control reverse-transcription polymerase chain reaction for glyceraldehyde-3-phosphate dehydrogenase was performed as internal controls.

Statistical Analysis

Data were analyzed by the Student *t* test and are expressed as means ± standard deviation. *P* values less than .05 were considered significant.

See the Supplementary Materials and Methods section and Supplementary Table 1 for details of vector construction and site-directed mutagenesis, lentiviral short hairpin RNA (shRNA) cloning and infection, recombinant protein, kinase assay, and microarray.

Results

Wnt Signaling Is Insufficient for mTORC1 Activation in Intestinal Polyps

We previously showed that the known upstream effectors of mTORC1, namely the phosphatidylinositol-3K/Akt pathway, MAPK/Erk kinase (Mek)/Extracellular signal-regulated kinase (Erk) pathway, and energy status were not directly involved in mTORC1 pathway activation in the intestinal polyps of $Apc^{\Delta 716}$ mice,[6] suggesting an alternative pathway(s) that activates mTORC1 signaling in the polyp adenomas. Because formation of the intestinal polyps in $Apc^{\Delta 716}$ mice is initiated by activation of Wnt signaling through homozygous loss of *Apc*,[15] we first determined whether Wnt signaling activation was sufficient for mTORC1 activation in the polyps. We stained for β-catenin and for the phosphorylated form of ribosomal S6 protein, a substrate of p70S6K downstream of mTORC1. We found strong β-catenin staining in the cytoplasm and nuclei of adenoma epithelial cells, including those in nascent polyps, but not in normal intestinal epithelial cells, indicating Wnt signal activation specifically in the tumor epithelium (Figure 1*A*). On the other hand, S6 was phosphorylated in the adenoma epithelium of only large polyps (>1.0 mm diameter), but not in the nascent ones (<0.5 mm) (Figure 1*B*). These results indicate that Wnt signaling induced by the loss of *Apc* gene does not lead to instant activation of mTORC1 signaling. Consistently, siRNA-mediated knockdown of *APC* in RKO cells, a colon cancer cell line in which Wnt signaling was not activated, failed to increase the phosphorylation level of S6K (Supplementary Figure 1*A*), despite that it increased the levels of β-catenin protein and mRNAs for Wnt target genes *cyclin D1* (*CCND1*) and *c-myc* (*MYC*) (Supplementary Figure 1*A* and *B*). These results indicate that Wnt signaling activation alone is insufficient for the mTORC1 signaling activation.

Tumor Size-Dependent Activation of JNK and mTORC1 Signaling in Intestinal Polyps

Because JNK was implicated in both mTORC1 signaling and intestinal tumorigenesis as described earlier, we next assessed the activation status of JNK signaling in the polyps of $Apc^{\Delta 716}$ mice by immunostaining for phospho-c-Jun (p-c-Jun), a representative substrate of JNK. Interestingly, c-Jun was phosphorylated in the adenoma cell nuclei of large polyps, but not in those of nascent ones (Figure 1*C*), reminiscent of the staining pattern for p-S6 (Figure 1*B*). Consistently, a Western blot analysis showed polyp size-dependent phosphorylation of JNK and c-Jun, as well as of S6 and 4EBP1, the downstream effectors of mTORC1 (Figure 1*D*). These results suggest that JNK signaling may be associated with the mTORC1 activation in intestinal tumors. To determine whether mTORC1 signaling was affected by JNK signaling, we treated $Apc^{\Delta 716}$ mice with the JNK inhibitor SP600125. Dosing with SP600125 markedly reduced the phosphorylation levels of S6K and S6, as well as those of JNK and c-Jun in the polyps as compared with the vehicle control (Figure 1*E* and *F*). These results indicate that activation of JNK is necessary for the mTORC1 signaling activation in the polyps of $Apc^{\Delta 716}$ mice.

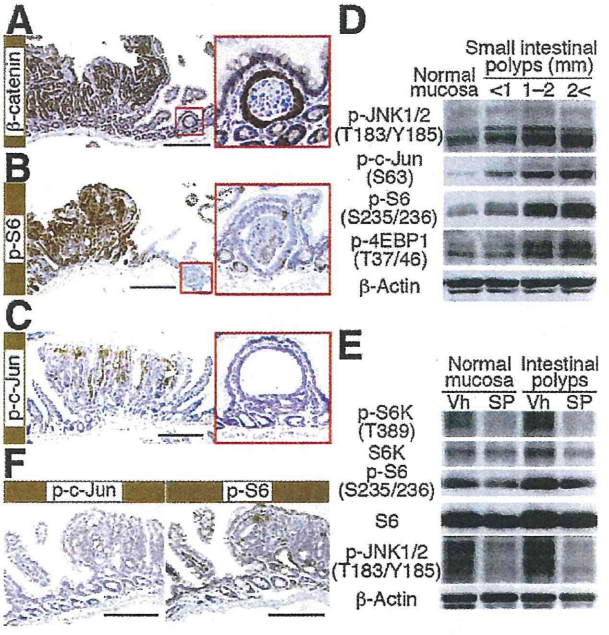

Figure 1. Activation of JNK and mTORC1 signaling in $Apc^{\Delta 716}$ mouse polyps. (*A–C*) Immunostaining for (*A*) β-catenin, (*B*) p-S6, and (*C*) p-c-Jun in intestinal polyps. (*D*) Western blot analysis for JNK and mTORC1 signaling in normal ileal mucosa and polyps of indicated sizes in $Apc^{\Delta 716}$ mice. Increased phosphorylation levels of JNK and c-Jun indicate JNK signaling, whereas those of S6 and 4EBP1 indicate mTORC1 activation. (*E*) Western blot analysis of mTORC1 signaling in intestinal polyps of SP600125-treated $Apc^{\Delta 716}$ mice. Vehicle (VH) or JNK inhibitor SP600125 (SP; at 50 mg/kg) was given for 2 weeks. (*F*) Immunostaining of p-c-Jun (left) and p-S6 (right) in intestinal polyps in SP600125-treated $Apc^{\Delta 716}$ mice. Bars: *A–C*, 500 μm; and *F*, 200 μm. Insets in *A–C* show subfields at 4-fold higher magnification.

Treatment With a JNK Inhibitor Blocks the Polyp Expansion in $Apc^{\Delta 716}$ Mice

Dosing $Apc^{\Delta 716}$ mice with the mTORC1 inhibitor RAD001 suppressed formation of intestinal tumors, especially those in the large size class (>1.5 mm).[6] We therefore hypothesized that treatment with JNK inhibitors might

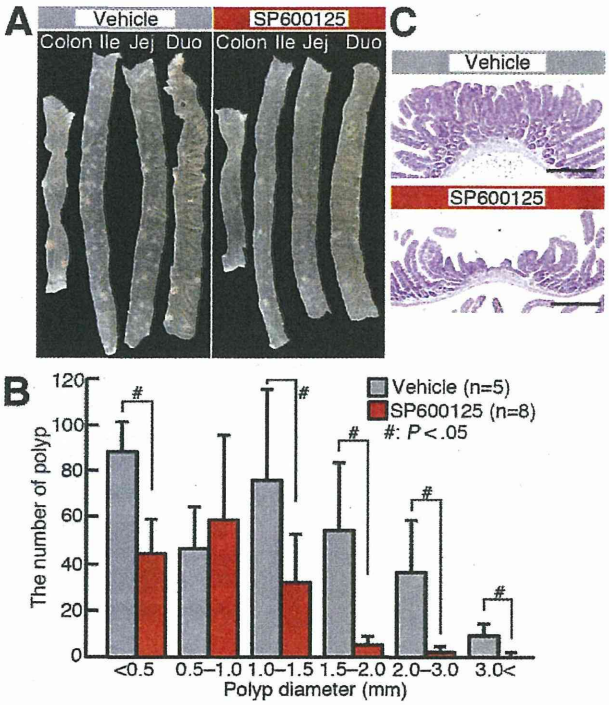

Figure 2. SP600125 suppresses polyp formation in $Apc^{\Delta 716}$ mice. (*A*) Gross appearance of intestinal polyps in $Apc^{\Delta 716}$ mice treated with vehicle or SP600125 at 50 mg/kg for 4 weeks. DUO, duodenum; JEJ, jejunum; ILE, ileum. (*B*) Size distribution of intestinal polyps in $Apc^{\Delta 716}$ mice treated with SP600125. (*C*) H&E-staining of polyps in vehicle- (left panel) or SP600125-treated (right panel) $Apc^{\Delta 716}$ mice. Bar, 500 μm.

have similar effects to those by inhibition of mTORC1. To test the possibility, we dosed $Apc^{\Delta 716}$ mice with the JNK inhibitor SP600125 (50 mg/kg) for 4 weeks. It significantly reduced the total number of intestinal polyps in $Apc^{\Delta 716}$ mice (mean ± standard deviation, 143.5 ± 69.4), compared with the vehicle control (mean ± standard deviation, 311.0 ± 68.8) (Figure 2*A* and *B*). Notably, the number of large polyps (>1.5 mm) was reduced dramatically in the SP600125-treated $Apc^{\Delta 716}$ mice (7.5 vs 99.8 [vehicle]) (Figure 2*B*). Interestingly, polyps in the SP600125-treated mouse showed a collapsed morphology at the top (Figure 2*C* and *D*), similar to those in the mTORC1 inhibitor-treated mice.[6] These results suggest that JNK signaling plays a key role in the intestinal tumorigenesis in $Apc^{\Delta 716}$ mice, upstream of the mTORC1 signaling.

JNK Activates mTORC1 Signaling Directly

Suppression of mTORC1 activation and of polyp formation by SP600125 in $Apc^{\Delta 716}$ mice suggests that JNK lies upstream of mTORC1 in vivo. To determine the role of JNK signaling in mTORC1, we treated colon cancer cell lines with JNK activator anisomycin or its inhibitor SP600125. As shown in Figure 3*A*, anisomycin increased the phosphorylation level of S6K in SW480 and HT29 cells, compared with the vehicle control (Figure 3*A*). On the other hand, SP600125 significantly reduced the phosphorylation of S6K in SW480 and HT29 cells (Figure 3*B*). Consistently, overexpression of JNK1, but not the kinase-dead JNK (K55R), increased the phosphorylation of both S6K and S6 protein (Supplementary Figure 2*A*), although neither of them affected the phosphorylation of Akt at Ser473, a residue implicated in Akt activation by mTORC2 (Supplementary Figure 2*A*). Likewise, shRNA-mediated knockdown of JNK decreased the phosphorylation level of S6K compared with the scramble RNA (Supplementary Figure 2*B*). These results suggest that the activation of JNK signaling is both necessary and sufficient for mTORC1 activation in colon cancer cells. We then investigated the mechanism by which JNK signaling activated mTORC1. We first tested whether JNK acted upstream or downstream of Rheb. Rheb is a small guanosine triphosphatase that can directly activate mTORC1.[17,18] As shown in Figure 3*C*, Rheb-induced S6K phosphorylation at Thr389 in SW480 cells was significantly inhibited by treatment with SP600125 (Figure 3*C*). Consistently, JNK knockdown by shRNA against JNK1/2 significantly reduced Rheb-induced S6K phosphorylation in SW480 cells (Figure 3*D*). These results suggest that JNK signaling affects mTORC1 at the downstream of Rheb.

JNK Up-Regulates mTORC1 Kinase Activity In Vitro

We then tested whether JNK could directly stimulate the mTORC1 kinase activity in vitro, using the mTOR immune complex prepared from 3-[(3-cholamidopropyl) dimethylammonio]-1-propanesulfonate (CHAPS)-solubilized cell lysates. As shown in Figure 3*E*, addition of the recombinant JNK1 significantly enhanced the mTORC1 kinase activity as determined by phosphorylation of the substrate 4EBP1 (Figure 3*E*). This enhancement was inhibited by RAD001, confirming the mTORC1-mediated phosphorylation of 4EBP1 (Figure 3*E*). Furthermore, the kinase-dead JNK1 showed significantly reduced mTORC1 activation compared with the wild-type JNK1 (Figure 3*F*), suggesting an essential role of the kinase activity in JNK1-mediated mTORC1 activation. The weak but significant activity of the kinase-dead JNK1 may be owing to co-purification of some proteins from the Sf9 insect cells that can activate mTORC1 in vitro, or to a kinase-independent function of JNK1, which remains to be investigated. Taken together, these results indicate that JNK can directly stimulate the mTORC1 kinase activity in vitro.

JNK Stimulates mTORC1 Through Phosphorylation of Raptor at Ser 863

Because JNK is a proline-directed serine/threonine kinase,[19] we hypothesized that JNK might activate mTORC1 through phosphorylation of an mTORC1 component at serine or threonine residues preceding proline. We searched for such sites in mTORC1 using PhosphoSitePlus (http://www.phosphosite.org/homeAction.do), and found 3 candidate residues (serines 567, 1859,

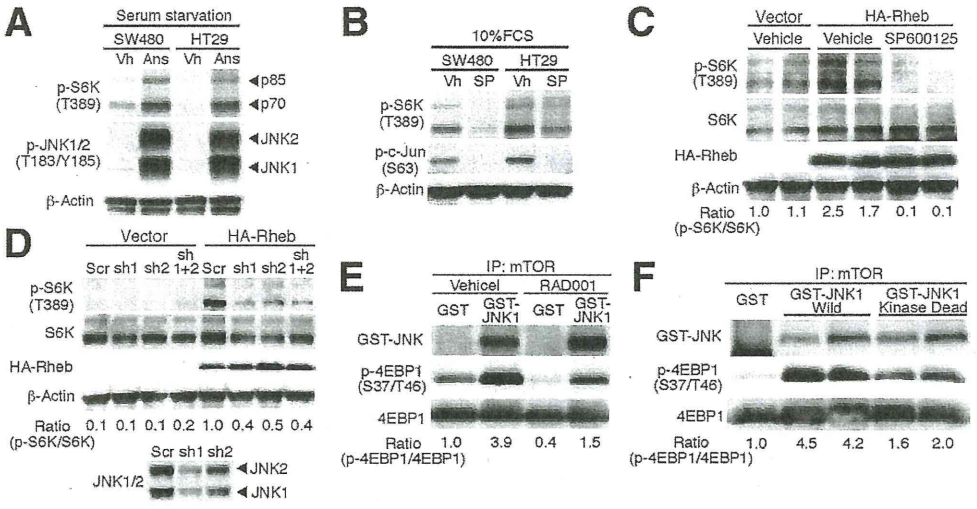

Figure 3. JNK signaling stimulates mTORC1 signaling. (*A*) Activation of JNK signaling stimulates mTORC1 signaling. Western blot analysis of p-S6K in colon cancer cell lines treated with JNK activator anisomycin (ANS; at 1 μg/mL) or vehicle control (VH) for 30 minutes. β-actin is shown as a loading control. (*B*) Inhibition of JNK signaling blocks mTORC1 signaling. Western blot analysis of p-S6K in colon cancer cell lines treated with SP600125 (SP; at 50 μmol/L) or vehicle (VH) for 6 hours. (*C*) SW480 cells transfected with HA-tagged ras homolog enriched in brain (Rheb) or vector control were starved in Dulbecco's PBS and treated with SP600125 (at 50 μmol/L) or vehicle for 30 minutes. (*D*) SW480 cells stably infected with shRNAs against JNK1/2 (sh1) or (sh2), either alone or in combination, or with scramble RNA (SCR). Cells were transfected with HA-Rheb or vector control, and starved for 30 minutes in D-PBS. Bottom panel shows successful knockdown of JNK1/2 by shRNA. (*E*) JNK activates mTORC1 in vitro. In vitro kinase assays were performed for mTORC1 with 4EBP1 as a substrate. mTORC1 was prepared from 293 cells treated with or without RAD001 by immunoprecipitation with an mTOR antibody. The immunoprecipitates were incubated with glutathione S-transferase (GST)-JNK or GST, and adenosine triphosphate for 20 minutes. 4EBP1 was added with or without 20 nmol/L RAD001, and the mixtures were incubated further for 30 minutes. Samples were subjected to Western blot analysis. (*F*) JNK kinase activity is required for activating mTORC1. mTORC1 in vitro kinase assays were performed with 4EBP1 as substrate. mTORC1 was prepared from 293 cells by immunoprecipitation with the mTOR antibody. The immunoprecipitates were incubated with GST-JNK (WILD) or GST-K55R, and adenosine triphosphate for 20 minutes. 4EBP1 was added and the mixtures were incubated further for 30 minutes. Samples were subjected to Western blot analysis.

and 1863) in mTOR itself and 2 candidate residues (serines 863 and 877) in Raptor, an essential component of mTORC1 (Supplementary Figure 3*A*). To determine whether JNK could phosphorylate mTOR or Raptor directly, we overexpressed myc-mTOR or myc-Raptor in 293T cells, and immunoprecipitated them from the cell lysate with an anti-myc antibody. Immune complex kinase assays showed that the recombinant JNK phosphorylated Raptor, but not mTOR in vitro (Figure 4*A*). To identify JNK phosphorylation sites in Raptor, we constructed mutant Raptor constructs with serine 863 or 877 substituted with alanine (S863A or S877A). As a control, we substituted the 3 serine phosphorylation sites for p90 ribosomal protein s6 kinase (RSK) at 719, 721, and 722 with alanine (AAA mutant).[20] In vitro kinase assays showed that the S863A mutation greatly reduced phosphorylation of Raptor by JNK, although it phosphorylated wild-type (WT) Raptor as well as the AAA and S877A mutants (Figure 4*B*). In vitro kinase assays using a recombinant Raptor fragment confirmed direct phosphorylation of Raptor by JNK at serine 863 (Figure 4*C*). To determine the role of Raptor phosphorylation at serine 863 in mTORC1 activation by JNK, we next performed kinase assays using myc-Raptor or myc-Raptor S863A overexpressed in SW480 cells. As shown in Figure 4*D*, JNK failed to enhance the kinase activity of mTORC1 (determined by 4EBP1 phosphorylation) containing myc-Raptor S863A, suggesting that phosphorylation of Raptor at serine 863 is essential for the JNK-mediated mTORC1 activation. Phosphorylation of Raptor at serine 863 was indeed increased in the intestinal polyps of $Apc^{\Delta 716}$ mice compared with normal mucosa (Supplementary Figure 3*B*). These results indicate that JNK stimulates mTORC1 signaling through phosphorylation of Raptor at serine 863, and thereby enhances intestinal polyp expansion in $Apc^{\Delta 716}$ mice.

JNK Up-Regulates Cyclin E in Intestinal Tumor Cells Through Two Distinct Mechanisms

We previously showed that the cyclin E protein level was reduced significantly in the intestinal polyps of $Apc^{\Delta 716}$ mice treated with RAD001.[6] Consistent with the role of JNK in mTORC1 activation in intestinal tumors, stimulation of the serum-starved HT29 cells with JNK activator anisomycin or 10% fetal calf serum (positive control) increased the level of cyclin E protein (Figure 5*A*), which was inhibited by treatment with RAD001 (Figure 5*A*). Importantly, anisomycin failed to enhance cyclin E protein level in JNK-knockdown HT29 cells

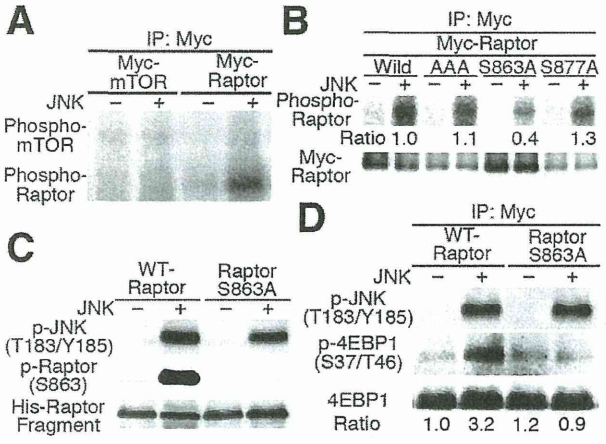

Figure 4. JNK directly activates mTORC1 through Raptor phosphorylation. (*A*) JNK phosphorylates Raptor, but not mTOR. In vitro kinase assays for JNK with immunoprecipitated mTOR or Raptor as substrate. mTOR or Raptor was prepared from 293T cells overexpressing myc-mTOR or myc-Raptor by immunoprecipitation with a myc antibody. The immunoprecipitates were incubated with or without recombinant glutathione S-transferase (GST)–JNK. [γ-^{32}P]Adenosine triphosphate was added and the mixtures were incubated for 30 minutes. Phosphorylation was detected by autoradiography. (*B*) JNK phosphorylates Raptor at serine 863. In vitro kinase assays for JNK using Raptor mutants as substrate. The Raptor protein was immunoprecipitated with myc antibody from 293T cells overexpressing myc-tagged WT or mutant Raptor. The immunoprecipitates were incubated with or without recombinant GST-JNK. [γ-^{32}P]Adenosine triphosphate was added and the mixtures were incubated for 30 minutes. Phosphorylation was detected by autoradiography. (*C*) In vitro kinase assay for JNK using recombinant Raptor fragment (amino acids 668~938) as substrate. A His-tagged recombinant Raptor protein was incubated with or without recombinant GST-JNK. Adenosine triphosphate was added and incubated for 30 minutes. Phosphorylation of Raptor at serine 863 was detected with p-Raptor (S863) antibody. Recombinant GST-JNK and His-tagged Raptor were detected by anti–p-JNK antibody and anti–His-tag antibodies, respectively. (*D*) Serine 863 of Raptor is important for mTORC1 activation. In vitro kinase activity was assayed for mTORC1 using 4EBP1 as substrate. mTORC1 containing WT- or S863A-Raptor was prepared from SW480 cells overexpressing myc-WT– or myc-S863A–Raptor by immunoprecipitation with myc-antibody. The immunoprecipitates were incubated with recombinant JNK and adenosine triphosphate for 20 minutes, and then 4EBP1 was added. The mixtures were incubated for an additional 30 minutes and then subjected to Western blot analysis.

(Figure 5*A*). These results suggested that increased cyclin E protein level was caused by JNK activation through mTORC1 signaling. We then tested whether JNK signaling would affect the cyclin E mRNA level. Treatment with anisomycin, as well as with 10% fetal calf serum, significantly increased the level in HT29 cells (Figure 5*B*). However, RAD001 did not affect the cyclin mRNA induction by anisomycin or fetal calf serum. An siRNA against c-Jun also reduced the level significantly in HT29 cells compared with a scramble RNA-treated control (Figure 5*C*). These results suggest that JNK activation in intestinal tumors enhances cyclin E expression through 2 mechanisms: by increasing the mRNA level via activation of c-Jun, a RAD001-insensitive pathway, and through increasing the protein level via mTORC1 activation, a RAD001-sensitive pathway.

JNK/mTORC1 Signaling Increases the Levels of Proliferin and Osteopontin in Intestinal Polyps of $Apc^{\Delta 716}$ *Mice*

The earlier results suggest that JNK activation can contribute to intestinal tumor expansion by 2 mechanisms. Because intestinal tumorigenesis is induced by Wnt signaling, we have determined whether JNK affects expression of Wnt target genes in a similar manner. Target genes common to Wnt and JNK pathway include *c-Myc*, *Mmp7*, *Cd44*, *osteopontin*, *Wnt2*, and *proliferin*.[21–24] Microarray analysis showed an extremely high level of *proliferin* mRNA in the polyps compared with normal mucosa (>900-fold), whereas the mRNA levels for *Mmp7*, *c-Myc*, and *osteopontin* were increased moderately (>2-fold). On the other hand, *Cd44* expression was increased only slightly (>1.3-fold), and *Wnt2* expression was undetectable (Supplementary Table 1). Although the level of proliferin protein was increased in the intestinal polyps compared with normal mucosa, RAD001 treatment reduced it to that of normal mucosa (Supplementary Figure 4*A* and *B*). The protein levels of osteopontin, c-Myc, and Mmp7 also were increased in the polyps compared with normal mucosa. Although RAD001 markedly reduced the level of osteopontin, that of Mmp7 or c-Myc was not affected significantly (Supplementary Figure 4C). Notably, SP600125 significantly reduced the mRNA and protein levels of both proliferin and osteopontin in the

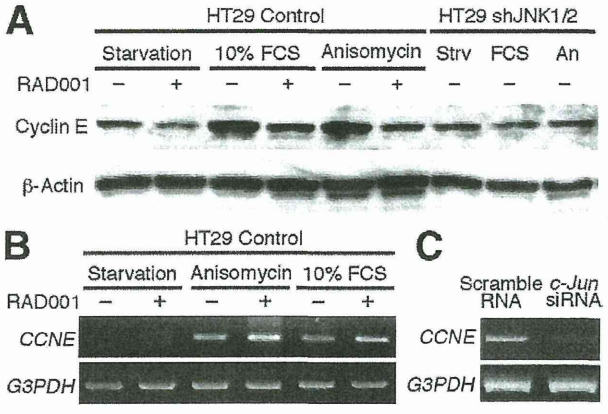

Figure 5. JNK signaling affects cyclin E at both protein and mRNA levels. (*A*) Western blot analysis for cyclin E protein level in HT29 cells treated with JNK activator anisomycin (1 μg/mL), or with anisomycin and mTORC1 inhibitor RAD001 (20 nmol/L) for 2 hours. The cyclin E level was not affected by serum or anisomycin stimulation in JNK1/2 knocked-down HT29 cell. (*B*) Reverse-transcription polymerase chain reaction analysis of cyclin E mRNA in HT29 cells. Starved cells were stimulated with anisomycin (1 μg/mL) or 10% fetal calf serum (FCS) for 1 hour in the presence or absence of 20 nmol/L RAD001. (*C*) Reverse-transcription polymerase chain reaction analysis of cyclin E mRNA in HT29 cells transfected with siRNA against *c-Jun* or with scramble RNA.

polyps (Supplementary Figure 4*D* and *F*), whereas RAD001 had no effect on their expression (Supplementary Figure 4*E*). These results suggest that JNK increases expression of not only cyclin E, but also proliferin and osteopontin in intestinal tumor cells. Because proliferin and osteopontin are implicated in angiognesis[25,26] and metastasis,[27] respectively, JNK may enhance tumor formation by up-regulating these molecules.

Discussion

We showed earlier that mTORC1 signaling was activated constitutively in the intestinal polyps of $Apc^{\Delta 716}$ mice, and that intestinal tumorigenesis was suppressed significantly by treatment with the mTORC1 inhibitor RAD001, accompanied by reduced cyclin levels and inhibition of tumor angiogenesis.[6] We have shown here that JNK signaling stimulates intestinal tumorigenesis in $Apc^{\Delta 716}$ mice through activation of the mTORC1 signaling. Namely, Wnt signaling induced by loss of *Apc* is insufficient for mTORC1 signaling both in vivo and in vitro (Figure 1 and Supplementary Figure 1). We conclude that JNK plays an essential role in mTORC1 activation based on the following results. First, both JNK and mTORC1 showed tumor size-dependent activation (Figure 1*D*). Second, treatment with a JNK inhibitor blocked mTORC1 signaling and significantly reduced the number of large polyps (>1.5 mm diameter) in $Apc^{\Delta 716}$ mice (Figures 1*E* and 2), similar to treatment with an mTORC1 inhibitor. Third, studies using colon cancer cell lines showed JNK mediated mTORC1 activation whereas JNK inhibition suppressed it (Figure 3*A* and *B*).

JNK is known to be activated by stresses such as ultraviolet irradiation and hydrogen peroxide treatment.[28,29] The intestines are exposed to bacteria, mechanical stresses, and digestive juices that can activate JNK signaling (Supplementary Figure 5*A*). We have shown here that JNK promotes mTORC1 activation through direct phosphorylation of Raptor at serine 863. Although it remains unclear how mTORC1 activity is regulated by phosphorylation of Raptor, several groups recently have reported the roles of Raptor phosphorylation in mTORC1 activation. Namely, RSK stimulated by mitogen-activated protein kinase signaling phosphorylates Raptor at serines 719, 721, and 722, which increases the mTORC1 activity.[20] Raptor is phosphorylated also by mTOR at serine 863, which stimulates the mTORC1 activity.[30,31] Other links between mTORC1 and JNK also have been reported. For example, JNK can enhance the S6K kinase activity through phosphorylation of S6K at serine 411,[32] and mTORC1 signaling can stimulate JNK signaling indirectly.[33] These multiple mechanisms may cooperate to amplify the signal.

JNK signaling is frequently activated in colorectal cancer,[8,34] and has been implicated in cell proliferation rather than cell death in the intestines.[35,36] Studies using mouse models have shown that JNK signaling promotes normal epithelial cell proliferation and intestinal tumorigenesis.[11,37,38] Although it was reported that $Jnk1^{-/-}$ mice developed spontaneous intestinal tumors (<1 polyp per animal),[39] other groups did not find any tumors in the intestines of $Jnk1^{-/-}$ mice.[40] Colon cancer induction by a chemical carcinogen was not affected either by *Jnk1* or *c-Jun* gene disruption in the intestinal epithelium.[40]

Our present results suggest that the JNK/mTORC1 signaling axis enhances intestinal tumorigenesis in $Apc^{\Delta 716}$ mice by promoting proliferation of tumor cells initiated by Wnt signaling. Activation of mTORC1 signaling by JNK may help increase translation of some mRNAs involved in tumor cell proliferation. We have found that protein levels of cyclin E, proliferin, and osteopontin were reduced by RAD001 (Figure 5 and Supplementary Figure 4), suggesting a role of mTORC1 in the biosynthesis of these proteins. Interestingly, the levels of mRNA for these molecules were reduced significantly by knockdown of c-Jun or by SP600125 (Figure 5 and Supplementary Figure 4*E*), indicating that JNK stimulates their transcription through c-Jun. Thus, JNK may induce expression of some proteins involved in tumor growth by 2 mechanisms: by promoting transcription via c-Jun phosphorylation, and by enhancing mRNA translation via mTORC1 activation (Supplementary Figure 5*B*).

Supplementary Material

Note: To access the supplementary material accompanying this article, visit the online version of *Gastroenterology* at www.gastrojournal.org, and at doi: 10.1053/j.gastro.2011.02.007.

References

1. Guertin DA, Sabatini DM. Defining the role of mTOR in cancer. Cancer Cell 2007;12:9–22.
2. Laplante M, Sabatini DM. mTOR signaling at a glance. J Cell Sci 2009;122:3589–3594.
3. Hudes G, Carducci M, Tomczak P, et al. Temsirolimus, interferon alfa, or both for advanced renal-cell carcinoma. N Engl J Med 2007;356:2271–2281.
4. Mother RJ, Scudder B, Oudard S, et al. Efficacy of everolimus in advanced renal cell carcinoma: a double-blind, randomised, placebo-controlled phase III trial. Lancet 2008;372:449–456.
5. Easton JB, Houghton PJ. mTOR and cancer therapy. Oncogene 2006;25:6436–6446.
6. Fujishita T, Aoki K, Lane HA, et al. Inhibition of the mTORC1 pathway suppresses intestinal polyp formation and reduces mortality in $Apc^{\Delta 716}$ mice. Proc Natl Acad Sci U S A 2008;105:13544–13549.
7. Wagner EF, Nebrada AR. Signal integration by JNK and p38 MAPK pathways in cancer development. Nat Rev Cancer 2009;9:537–549.
8. Licato LL, Brenner DA. Analysis of signaling protein kinases in human colon or colorectal carcinomas. Dig Dis Sci 1998;43:1454–1464.
9. Sakurai T, Maeda S, Chang L, et al. Loss of hepatic NF-κB activity enhances chemical hepatocarcinogenesis through sustained c-Jun N-terminal kinase 1 activation. Proc Natl Acad Sci U S A 2006;103:10544–10551.

10. Shibata W, Maeda S, Hikiba Y, et al. c-Jun NH2-terminal kinase 1 is a critical regulator for the development of gastric cancer in mice. Cancer Res 2008;68:5031–5039.
11. Nateri AS, Spencer-Dene B, Behrens A. Interaction of phosphorylated c-Jun with TCF4 regulates intestinal cancer development. Nature 2005;437:281–285.
12. Shima H, Pende M, Chen Y, et al. Disruption of the p70(s6k)/p85(s6k) gene reveals a small mouse phenotype and a new functional S6 kinase. EMBO J 1998;17:6649–6659.
13. Hirosumi J, Tuncman G, Chang L, et al. A central role for JNK in obesity and insulin resistance. Nature 2002;420:333–336.
14. Belgardt BF, Mauer J, Wunderlich FT, et al. Hypothalamic and pituitary c-Jun N-terminal kinase 1 signaling coordinately regulates glucose metabolism. Proc Natl Acad Sci U S A 2010;107:6028–6033.
15. Oshima M, Oshima H, Kitagawa K, et al. Loss of *Apc* heterozygosity and abnormal tissue building in nascent intestinal polyps in mice carrying a truncated *Apc* gene. Proc Natl Acad Sci U S A 1995;92:4482–4486.
16. Verma UN, Surabhi RM, Schmaltieg A, et al. Small interfering RNAs directed against β-catenin inhibit the in vitro and in vivo growth of colon cancer cells. Clin Cancer Res 2003:9:1291–1300.
17. Inoki K, Li Y, Xu T, et al. Rheb GTPase is a direct target of TSC2 GAP activity and regulates mTOR signaling. Genes Dev 2003;17:1829–1834.
18. Long X, Lin Y, Ortiz-Vega S, et al. Rheb binds and regulates the mTOR kinase. Curr Biol 2005;15:702–713.
19. Cano E, Mahadevan LC. Parallel signal processing among mammalian MAPKs. Trends Biochem Sci 1995;20:117–122.
20. Carrière A, Cargnello M, Julien LA, et al. Oncogenic MAPK signaling stimulates mTORC1 activity by promoting RSK-mediated raptor phosphorylation. Curr Biol 2008;18:1269–1277.
21. Saadeddin A, Babaei-Jadidi R, Spencer-Dene B, et al. The links between transcription, β-catenin/JNK signaling, and carcinogenesis. Mol Cancer Res 2009;7:1189–1196.
22. Ziegler S, Röhrs S, Tickenbrock L, et al. Novel target genes of the Wnt pathway and statistical insights into Wnt target promoter regulation. FEBS J 2005;272:1600–1615.
23. Shaulian E, Karin M. AP-1 as a regulator of cell life and death. Nat Cell Biol 2002;4:E131–E136.
24. Groskopf JC, Linzer DI. Characterization of a delayed early serum response region. Mol Cell Biol 1994;14:6013–6020.
25. Jackson D, Volpert OV, Bouck N, et al. Stimulation and inhibition of angiogenesis by placental proliferin and proliferin-related protein. Science 1994;266:1581–1584.
26. Toft DJ, Rosenberg SB, Bergers G, et al. Reactivation of proliferin gene expression is associated with increased angiogenesis in a cell culture model of fibrosarcoma tumor progression. Proc Natl Acad Sci U S A 2001;98:13055–13059.
27. Irby RB, McCarthy SM, Yeatman TJ. Osteopontin regulates multiple functions contributing to human colon cancer development and progression. Clin Exp Metastasis 2004;21:515–523.
28. Johnson GL, Nakamura K. The c-jun kinase/stress-activated pathway: regulation, function and role in human disease. Biochim Biophys Acta 2007;1773:1341–1348.
29. Ruffels J, Griffin M, Dickenson JM. Activation of ERK1/2, JNK and PKB by hydrogen peroxide in human SH-SY5Y neuroblastoma cells: role of ERK1/2 in H_2O_2-induced cell death. Eur J Pharmacol 2004;483:163–173.
30. Wang L, Lawrence JC Jr, Sturgill TW, et al. Mammalian target of rapamycin complex 1 (mTORC1) activity is associated with phosphorylation of raptor by mTOR. J Biol Chem 2009;284:14693–14697.
31. Foster KG, Acosta-Jaquez HA, Romeo Y, et al. Regulation of mTOR complex 1 (mTORC1) by raptor Ser^{863} and multisite phosphorylation. J Biol Chem 2010;285:80–94.
32. Zhang Y, Dong Z, Nomura M, et al. Signal transduction pathways involved in phosphorylation and activation of p70S6K following exposure to UVA irradiation. J Biol Chem 2001;276:20913–20923.
33. Panaretakis T, Hjortsberg L, Tamm KP, et al. Interferon α induces nucleus-independent apoptosis by activating extracellular signal-regulated kinase 1/2 and c-Jun NH_2-terminal kinase downstream of phosphatidylinositol 3-kinase and mammalian target of rapamycin. Mol Biol Cell 2008;19:41–50.
34. Licato LL, Keku TO, Wurzelmann JI, et al. In vivo activation of mitogen-activated protein kinases in rat intestinal neoplasia. Gastroenterology 1997;113:1589–1598.
35. Weston CR, Wong A, Hall JP, et al. The c-Jun NH_2-terminal kinase is essential for epidermal growth factor expression during epidermal morphogenesis. Proc Natl Acad Sci U S A 2004;101:14114–14119.
36. Yamagata H, Matsuzaki K, Mori S, et al. Acceleration of Smad2 and Smad3 phosphorylation via c-Jun NH_2-terminal kinase during human colorectal carcinogenesis. Cancer Res 2005;65:157–165.
37. Sancho R, Nateri AS, de Vinuesa AG, et al. JNK signalling modulates intestinal homeostasis and tumourigenesis in mice. EMBO J 2009;28:1843–1854.
38. Endo H, Hosono K, Fujisawa T, et al. Involvement of JNK pathway in the promotion of the early stage of colorectal carcinogenesis under high-fat dietary conditions. Gut 2009;58:1637–1643.
39. Tong C, Yin Z, Song Z, et al. c-Jun NH2-terminal kinase 1 plays a critical role in intestinal homeostasis and tumor suppression. Am J Pathol 2007;171:297–303.
40. Hasselblatt P, Gresh L, Kudo H, et al. The role of the transcription factor AP-1 in colitis-associated and β-catenin-dependent intestinal tumorigenesis in mice. Oncogene 2008;27:6102–6109.

Received October 10, 2010. Accepted February 1, 2011.

Reprint requests

Address requests for reprints to: Makoto M. Taketo, MD, PhD, Department of Pharmacology, Graduate School of Medicine, Kyoto University, Yoshida-Konoé-Cho, Sakyo-Ku, Kyoto 606-8501, Japan. e-mail: taketo@mfour.med.kyoto-u.ac.jp; fax: (81) 75-753-4402.

Acknowledgments

The authors thank P. M. McSheehy for RAD001; M. Oshima, T. Kitamura, M. Sonoshita, S. Arimura, F. Kakizaki, A. Deguchi, and K. Aoki for discussions; M. Tsujii for the SW480 cells; F. Tamanoi for HA-Rheb expression plasmid; and A. Matsunaga for microarray analysis. The authors also thank R. A. Weinberg for pLKO.1; D. Trono for psPAX2 and pMD2.G; and D. M. Sabatini for pLKO.1 scramble shRNA, myc–mammalian target of rapamycin, and myc-Raptor plasmids.

Current address of M.A.: Division of Molecular Pathology, Aichi Cancer Center Research Institute, 1-1, Kanokoden, Chikusa-Ku, Nagoya 464-8681, Japan.

M.A. and M.M.T. are co-senior authors.

Conflicts of Interest

The authors disclose no conflicts.

Funding

Supported by a Grant-in-Aid for Scientific Research from the Ministry of Education, Culture, Sports, Science and Technology of Japan (M.M.T.), and by a Grant-in-Aid for Cancer Research for the Third-Term Comprehensive 10-Year Strategy for Cancer Control from the Ministry of Health, Labour and Welfare of Japan (M.A.). T. F. is supported by the Global COE Program "Center for Frontier Medicine" by Ministry of Education, Culture, Sports, Science and Technology (MEXT), Japan. The experiments using radioisotopes were performed at the Radioisotope Research Center of Kyoto University.

Supplementary Materials and Methods

Vector Construction and Site-Directed Mutagenesis

The full-length, WT JNK1b1 complementary DNA (cDNA) was isolated by a polymerase chain reaction–based cloning technique from SW480 cells. The cDNA was inserted into myc-tag expression vector pCMV-Tag3B (Agilent Technologies, Santa Clara, CA). Site-directed mutagenesis for K55R was performed using the QuikChange site-directed mutagenesis kit (Agilent Technologies) with the following oligomers: forward: 5′-GAAAGAAATGTTGCAATCAgGAAGCTAAGCCGACCATTT-3′, and reverse: 5′-AAATGGTCGGCTTAGCTTCcTGATTGCAACATTTCTTTC-3′. The lower case letters indicate the mutated bases encoding the adenosine triphosphate (ATP)-binding site of JNK. Expression plasmids for Myc-mTOR (Addgene #1861) and Myc-Raptor (Addgene #1859) were purchased from Addgene (Cambridge, MA). HA-Rheb expression plasmid was provided by F. Tamanoi (University of California Los Angeles, Los Angeles, CA). Site-directed mutagenesis for Raptor S863A, S877A, and AAA (S719A, S721A, S722A) was performed using PrimeSTAR MAX (Takara, Otsu, Japan) with the following oligomers: Raptor S863A forward: 5′-CCCGCCgcCCCCACCAACAAGGGCGTG-3′, and reverse: 5′-GGTGGGGgcGGCGGGGGCCGACTGCGT-3′. Raptor S877A forward: 5′-GGGGGGCgCCCCTCCGGCGTCCAGCA-3′, and reverse: 5′-GGAGGGGcGCCCCCCGCCTGGTGGAT-3′. Raptor AAA forward: 5′-GTgCTGTGgcCgCCTATGGAAACATCCGTG-3′, and reverse: 5′-AGGcGgcCACAGcACGAAGTCTGGGGGTGCA-3′. The lower cases indicate the mutated bases in Raptor to introduce the serine to alanine substitutions.

Lentiviral shRNA Cloning

Desalted oligonucleotides were annealed and cloned into pLKO.1 (Addgene #8453). The sequences of the oligonucleotides are as follows: JNK1/2 shRNA_1 sense, 5′-CCGGAAAGAATGTCCTACCTTCTTTCTCGAGAAAGAAGGTAGGACATTCTTTTTTTTG-3′; JNK1/2 shRNA_1 antisense, 5′-AATTCAAAAAAAAGAATGTCCTACCTTCTTTCTCGAGAAAGAAGGTAGGACATTCTTT-3′; JNK1 shRNA_2 sense, 5′-CCGGAAGCTCCACCACCAAAGATCCCTCGAGGGATCTTTGGTGGTGGAGCTTTTTTTTG-3′; JNK1 shRNA_2 antisense, 5′-AATTCAAAAAAAGCTCCACCACCAAAGATCCCTCGAGGGATCTTTGGTGGTGGAGCTT-3′; JNK2 shRNA_2 sense, 5′-CCGGAAGGCACTGACCATATTGATCCTCGAGGATCAATATGGTCAGTGCCTTTTTTTG-3′; and JNK2 shRNA_2 antisense, and 5′-AATTCAAAAAAAGGCACTGACCATATTGATCCTCGAGGATCAATATGGTCAGTGCCTT-3′.

Lentivirus Production and Infection

For packaging, psPAX2 (Addgene #12260) and pMD2.G (Addgene #12259) were co-transfected with pLKO.1 containing the insert for scramble shRNA (Addgene plasmid #1864) or *JNK* shRNA of pLKO.1 into 293T cells by using Lipofectamine 2000 (Invitrogen). Virus-containing media were harvested 48 hours after transfection, and filtered through a sterile 0.45-micron filter (Millipore). Cells were infected with the virus stocks in the presence of 8 μg/mL polybrene (Millipore), and selected for puromycin resistance.

Recombinant JNK1 Protein

Glutathione S-transferase (GST)-tagged recombinant fusion proteins of WT- and K55R-human JNK1b1 were produced by a baculovirus expression system. JNK1b1 cDNA was inserted into pENTER 3C vector (Invitrogen). After recombination of JNK1 cDNA from pENTER 3C to pDEST 20 (Invitrogen), WT- or K55R-JNK1 pDEST 20 vector was transfected into Sf9 cells with Cellfectin reagent (Invitrogen). After amplification of the recombinant baculoviruses, fusion proteins were purified from the lysates of infected Sf9 cells using glutathione sepharose (GE Healthcare UK Ltd, Buckinghamshire, UK) from the recombinant baculovirus-infected Sf9 cells.

Kinase Assay for mTORC1

The mTORC1 complex was prepared from 293 cells. Cells were lysed in lysis buffer A (40 mmol/L HEPES [pH 7.4], 120 mmol/L NaCl, 1 mmol/L ethylenediaminetetraacetic acid [EDTA], 0.3% CHAPS, 10 mmol/L sodium pyrophosphate, 10 mmol/L NaF, and 1.5 mmol/L Na_3VO_4). The lysate was centrifuged at 14,000 × g for 5 minutes at 4°C, and the supernatant was incubated with anti-mTOR antibody (IBL) for 3 hours at 4°C, and incubated with protein G–agarose beads for 1 hour. The beads were washed 3 times with lysis buffer A, and once with kinase buffer A (25 mmol/L HEPES [pH 7.4], 50 mmol/L NaCl, 10 mmol/L $MnCl_2$, 10 mmol/L $MgCl_2$, and 50 mmol/L β-glycerophosphate). Kinase assays were performed at 30°C for 30 minutes in kinase buffer A with 200 μmol/L ATP, and 1 μg of 4EBP1 (Biomol, Plymouth Meeting, PA). Where indicated, the mixture was pretreated with 200 ng of recombinant JNK1 (Cell Signaling Technology), GST-WT-JNK1, or GST-K55R-JNK1 as described earlier. The reactions were terminated with 2× sample buffer. The phosphorylation level of 4EBP1 in samples was determined by Western blot analysis.

Kinase Assay for JNK using radioactive isotopes

Myc-tagged mTOR, WT-Raptor, Raptor S863A, Raptor S877A, and Raptor AAA proteins were overexpressed in 293T cells by transformation using Lipofectamine 2000. The cells were lysed in lysis buffer B (20 mmol/L Tris [pH 7.4], 150 mmol/L NaCl, 1 mmol/L EDTA, 1 mmol/L ethylene glycol bis(2-aminoethyl ether)-*N,N,N′,N′*-tetraacetic acid, 2% Triton-X100, 2.5 mmol/L sodium pyrophosphate, 1 mmol/L β-glycerophosphate, 1 mmol/L Na_3VO_4, and 1 μg/mL leupeptin). The lysate was

spun at 14,000 × g for 5 minutes at 4°C, and the supernatant was incubated with anti-myc antibody–conjugated agarose beads (Nacalai Tesque, Kyoto, Japan) overnight at 4°C. The beads were washed 3 times with lysis buffer B, and once with kinase buffer B (25 mmol/L Tris [pH 7.5], 5 mmol/L β-glycerophosphate, 2 mmol/L dithiothreitol, 0.1 mmol/L Na_3VO_4, and 10 mmol/L $MgCl_2$). Kinase assays were performed at 30°C for 30 minutes in kinase buffer B with 100 μmol/L cold ATP, and 200 kBq of [γ-^{32}P]ATP (PerkinElmer, Waltham, MA) with or without 200 ng/50 μL of JNK1 (Cell Signaling Technology). The reactions were terminated with 2× sample buffer. The samples were loaded on sodium dodecyl sulfate–polyacrylamide gel electrophoresis, and the dried gel was analyzed by a BAS 1800 II phosphoimager (Fujifilm, Tokyo, Japan).

Raptor Protein Fragment for JNK Kinase Assay

Bacterial expression vector for 6xHistidine-tagged WT- and S863A-Raptor (His-Raptor) were prepared by inserting human Raptor cDNA fragment (a.a. 668–938) into pET15b vector (Novagen, Madison, WI). BL21 *Escherichia coli* cells (BL21 Star [DE3]; Invitrogen) containing pET15b-His-Raptor were grown in LB medium with ampicillin and induced with 1 mmol/L isopropyl-β-D-thiogalactopyranoside for 4 hours at 30°C. The fusion proteins were purified with Ni-NTA His-Binds resins according to the manufacturer's protocol (Novagen). Kinase assays were performed at 30°C for 30 minutes in kinase buffer B with 200 μmol/L ATP, 1 μg of 6xHistidine-tagged WT- or S863A-Raptor protein, with or without 200 ng/50 μL of JNK1. The reactions were terminated with 2× sample buffer. The phosphorylation level of Raptor at Ser863 was determined by Western blot analysis with p-Raptor S863 antibody (Santa Cruz).

Supplementary Table 1. Gene Expression Profiles Analyzed by DNA Microarrays in Intestinal Polyps

	Gene	ID	Increased
1	*Proliferin*	NM_031191.1	906.82
2	*Il1rl1*	NM_001025602.2	125.51
3	*Phlda1*	NM_009344.3	122.82
4	*Atf1*	NM_007497.3	87.44
5	*Zfp62*	NM_009562.2	70.23
6	*Hbb-b2*	NM_016956.2	67.28
7	*Expi*	NM_007969.4	63.75
8	*Thbs1*	NM_011580.3	56.31
9	*Cfi*	NM_007686.2	55.64
10	*Foxq1*	NM_008239.4	50.75
11	*Me1*	NM_008615.2	46.94
12	*Pkd2*	NM_008861.3	46.06
13	*Gja1*	NM_010288.3	45.96
14	*Ctse*	NM_007799.3	45.49
15	*Gch1*	NM_008102.3	43.19
16	*Lmna*	NM_019390.2	41.71
17	*Rbp1*	NM_011254.5	41.61
18	*Hnrnpa1*	NM_010447.4	40.11
19	*Amd2*	NM_007444.3	36.23
20	*Hif1a*	NM_010431.2	35.61
21	*Morf4l2*	NM_001168225.1	35.31
22	*Kif5b*	NM_008448.3	33.85
23	*Rev3l*	NM_011264.3	33.77
24	*Ptpro*	NM_001164402.1	31.41
25	*Ube2e1*	NM_009455.3	30.94
26	*D030029J20Rik*	AW228840	30.55
27	*Mmp10*	NM_019471.2	29.52
28	*Marcks*	NM_008538.2	29.43
29	*Procr*	NM_011171.2	28.66
30	*Hars*	NM_008214.4	28.48
31	*Matr3*	NM_010771.6	27.82
32	*Dck*	NM_007832.4	27.48
33	*Cbx3*	NM_007624.3	27.26
34	*Tfdp1*	NM_009361.2	26.53
35	*A030003K02Rik*	AW124129	25.92
36	*Ctcf*	NM_181322.3	25.59
37	*Ranbp9*	NM_019930.2	25.48
38	*Hs3st1*	NM_010474.2	25.04
39	*Lrrc58*	NM_177093.3	24.35
40	*Il1rn*	NM_001039701.3	24.24
41	*Eftud2*	NM_011431.3	23.07
42	*Bub1*	NM_009772.2	23.06
43	*Pdgfra*	NM_011058.2	22.82
44	*Slc20a1*	NM_015747.2	22.79
45	*Hivep1*	NM_007772.2	22.66
46	*Cetn3*	NM_007684.3	22.26
47	*F3*	NM_010171.3	22.11
48	*Cxcl5*	NM_009141.2	22.10
49	*Amot*	NM_153319.2	21.95
50	*Strap*	NM_011499.3	21.60
51	*Ppic*	NM_008908.4	21.40
52	*Psmb5*	NM_011186.1	21.05
53	*Adh5*	NM_007410.2	20.62
54	*Fkbp1a*	NM_008019.2	20.41
55	*Kitl*	NM_013598.2	20.37
56	*H2afz*	NM_016750.2	20.30
57	*Syncrip*	NM_019666.2	20.20
58	*Robo1*	NM_019413.2	20.05
59	*Cxcr7*	NM_007722.3	19.90
60	*Galnt3*	NM_015736.2	19.51
61	*Atp6v1c1*	NM_025494.3	19.19

Supplementary Table 1. Continued

	Gene	ID	Increased
62	*Mcpt1*	NM_008570.1	18.77
63	*Snd1*	NM_019776.2	18.70
64	*Hells*	NM_008234.3	18.62
65	*T*	NM_009309.2	18.42
66	*Gpi1*	NM_008155.3	18.11
67	*Hmgb2*	NM_008252.3	18.09
68	*Smarca2*	NM_026003.2	18.02
69	*Anxa1*	NM_010730.2	18.00
70	*Hnrnph1*	NM_021510.2	17.90
71	*Tra2b*	NM_009186.4	17.18
72	*Blnk*	NM_008528.4	17.06
73	*Stra6*	NM_001162475.1	17.02
74	*Fkbp9*	NM_012056.2	17.02
75	*Wbp5*	NM_011712.2	17.02
76	*Ehf*	NM_007914.3	16.92
77	*Ddx3x*	NM_010028.3	16.74
78	*Plat*	NM_008872.2	16.56
79	*Ptp4a1*	NM_011200.2	16.34
80	*Tmem131*	NM_018872.2	16.34
81	*Odf2*	NM_001113213.1	16.09
82	*Slc7a5*	NM_011404.3	16.08
83	*Sc5d*	NM_172769.2	16.01
84	*Dfna5*	NM_018769.3	15.94
85	*Nucks1*	NM_001145804.1	15.77
86	*Pcna*	NM_011045.2	15.75
87	*Uba2*	NM_016682.2	15.69
88	*Rbbp7*	NM_009031.3	15.59
89	*Hspd1*	NM_010477.4	15.50
90	*Sox17*	NM_011441.4	15.43
91	*Cdc6*	NM_011799.2	15.42
92	*Cct7*	NM_007638.4	15.38
93	*2610201A13Rik*	AA222883	15.20
94	*Rab18*	NM_181070.5	15.19
95	*Ctsl*	NM_009984.3	15.14
96	*Tsc22d1*	NM_009366.2	14.89
97	*Rcn2*	NM_011992.2	14.86
98	*Brd1*	NM_001033274.3	14.82
99	*Clcn3*	NM_007711.3	14.70
100	*Ptn*	NM_008973.2	14.62
101	*Cma1*	NM_010780.2	14.60
102	*Rbm14*	NM_019869.2	14.51
103	*Chrnb1*	NM_009601.4	14.35
104	*Rps6ka4*	NM_019924.1	14.31
105	*Rbbp4*	NM_009030.3	14.29
106	*Ptma*	NM_008972.2	14.23
107	*Krt6a*	NM_008476.3	14.10
108	*Tnfrsf11b*	NM_008764.3	14.10
	Spp1	NM_009263.2	4.96
	Mmp7	NM_001177352.1	3.07
	Myc	NM_021330.4	2.65
	Cd44	NM_001039150.1	1.38

NOTE. mRNA preparations from the polyps and normal mucosa in the $Apc^{\Delta 716}$ mice were analyzed by DNA microarrays (Affymetrix). The data are expressed as fold-changes in the polyps of $Apc^{\Delta 716}$ mice compared with normal mucosa of $Apc^{\Delta 716}$ mice. Results show the mean (n = 3).

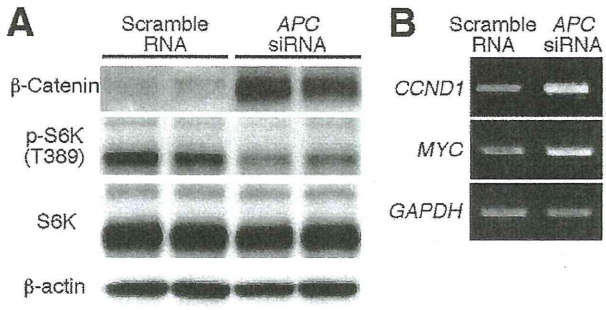

Supplementary Figure 1. mTORC1 signaling was unaffected by Wnt signaling induced by loss of Apc. (*A*) Western blot analysis of p-S6K in RKO colon cancer cells where Wnt signaling was intact and siRNA against *APC* or scramble RNA was treated. (*B*) reverse-transcription polymerase chain reaction (RT-PCR) analysis of Wnt target genes, *CCND1*, and *MYC* in RKO cells treated with siRNA against *APC* or scramble RNA. *Glyceraldehyde-3-phosphate dehydrogenase* is shown as a loading control.

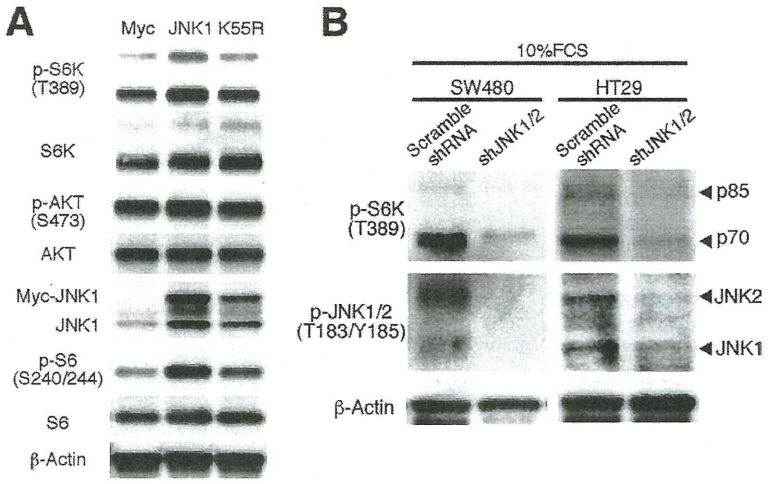

Supplementary Figure 2. JNK activates mTORC1 signaling. (*A*) Western blot analysis of mTORC1 signaling in SW480 cells overexpressing Myc-JNK1 or Myc-K55R. SW480 cells were incubated in a medium containing 10% fetal calf serum (FCS). (*B*) Western blot analysis of p-S6K in SW480 and HT29 cells expressing shRNA against JNK1/2 (sh1) or scramble RNA. Cells were incubated in a medium containing 10% FCS.

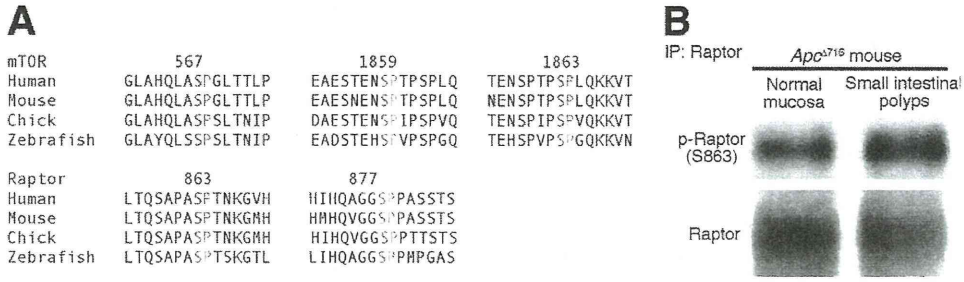

Supplementary Figure 3. JNK phosphorylates mTORC1 component Raptor. (*A*) Amino acid sequence alignments showing conservation of the possible JNK phosphorylation sites, serines, or threonines adjacent to prolines, of mTOR and Raptor orthologs in several species. (*B*) Phosphorylation of Raptor at serine 863 is increased in polyps of $Apc^{\Delta 716}$ mice. The Raptor protein from normal mucosa or polyps in the small intestine of $Apc^{\Delta 716}$ mice was prepared by immunoprecipitation and subjected to Western blot analysis.

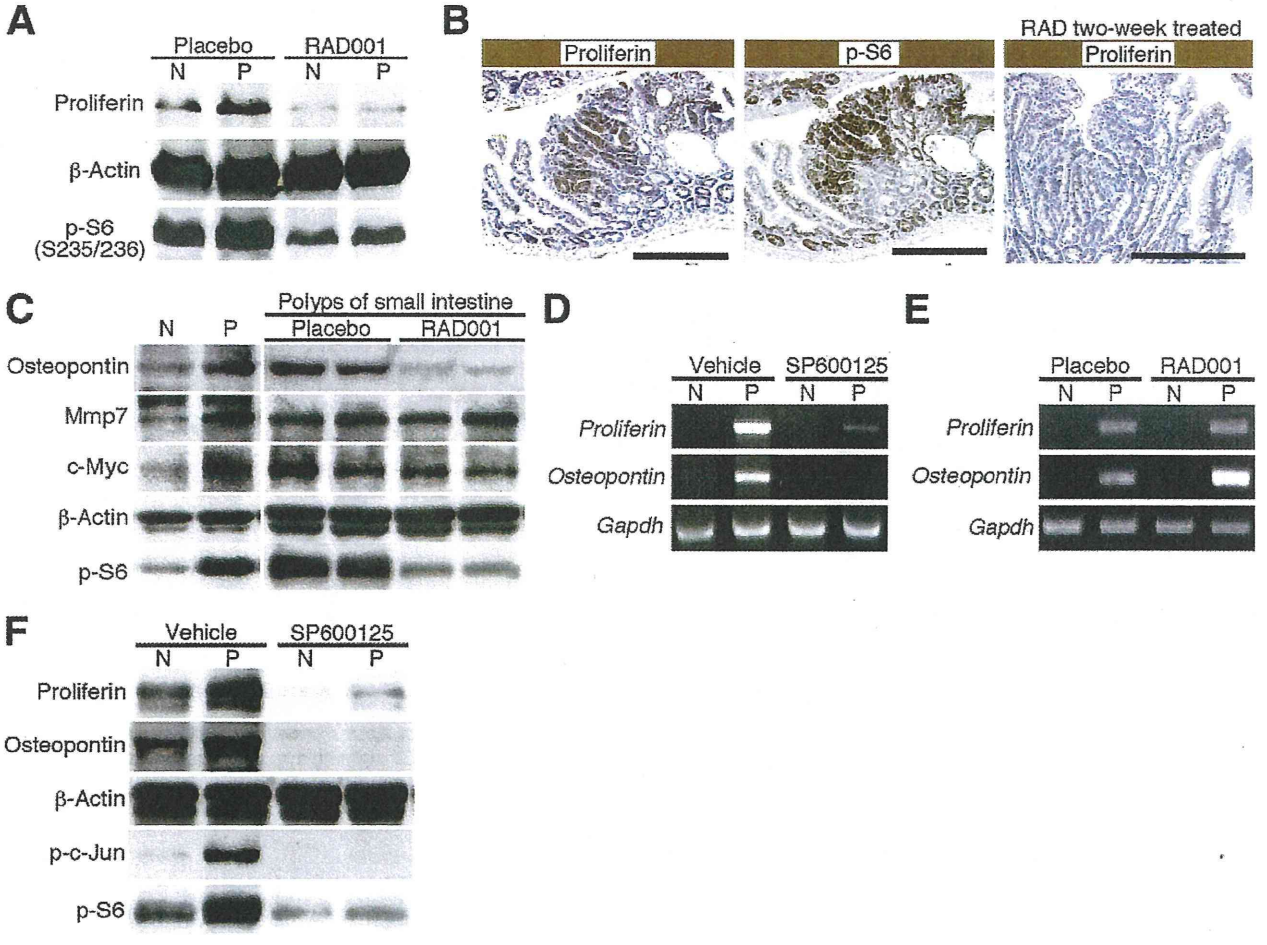

Supplementary Figure 4. JNK/mTOR signaling increased the levels of proliferin and osteopontin in the polyps of $Apc^{\Delta 716}$ mice. (*A*) Western blot analysis of proliferin in normal mucosa or polyps of the small intestine. $Apc^{\Delta 716}$ mice were treated with RAD001 at 10 mg/kg or with placebo for 2 weeks. N, normal mucosa; P, polyps. (*B*) Immunostaining for proliferin (left) and p-S6 (middle) in serial sections of $Apc^{\Delta 716}$ mouse polyp. (Right) Immunostaining for proliferin in a polyp of the $Apc^{\Delta 716}$ mouse treated with RAD001 for 2 weeks. (*C*) Western blot analysis of osteopontin, Mmp7, and c-Myc proteins in normal mucosa or polyps of the small intestine of $Apc^{\Delta 716}$ mice treated with 10 mg/kg RAD001 or with placebo for 2 weeks. N, normal mucosa; P, polyps. (*D*) Reverse-transcription polymerase chain reaction (RT-PCR) analysis of *proliferin* and *osteopontin* mRNAs in normal mucosa or polyps of the small intestine of $Apc^{\Delta 716}$ mice treated with the vehicle or with SP600125 at 50 mg/kg for 2 weeks. N, normal mucosa; P, polyps. (*E*) RT-PCR analysis showing that *proliferin* and *osteopontin* mRNAs in normal mucosa or polyps of the small intestine of $Apc^{\Delta 716}$ mice treated with the placebo or with RAD001 at 10 mg/kg for 2 weeks. N, normal mucosa; P, polyps. (*F*) Western blot analysis of proliferin and osteopontin in normal mucosa or polyps of the small intestine. $Apc^{\Delta 716}$ mice were treated with SP600125 at 50 mg/kg or with placebo for 2 weeks. N, normal mucosa; P, polyps.